


# *Cnp* Promoter-Driven Sustained ERK1/2 Activation Increases B-Cell Activation and Suppresses Experimental Autoimmune Encephalomyelitis

Marisa A. Jeffries<sup>1,2,3</sup> , Alison E. Obr<sup>1,3</sup> , Kelly Urbanek<sup>4</sup>, Sharyl L. Fyffe-Maricich<sup>2,4</sup> and Teresa L. Wood<sup>1,3</sup> 

ASN Neuro  
Volume 12: 1–18  
© The Author(s) 2020  
Article reuse guidelines:  
sagepub.com/journals-permissions  
DOI: 10.1177/1759091420971916  
journals.sagepub.com/home/asn  


## Abstract

The ERK1/2 signaling pathway promotes myelin wrapping during development and remyelination, and sustained ERK1/2 activation in the oligodendrocyte (OL) lineage results in hypermyelination of the CNS. We therefore hypothesized that increased ERK1/2 signaling in the OL lineage would 1) protect against immune-mediated demyelination due to increased baseline myelin thickness and/or 2) promote enhanced remyelination and thus functional recovery after experimental autoimmune encephalomyelitis (EAE) induction. *Cnp-Cre;Mek1DD-eGFP/+* mice that express a constitutively active form of MEK1 (the upstream activator of ERK1/2) in the OL lineage, exhibited a significant decrease in EAE clinical severity compared to controls. However, experiments using tamoxifen-inducible *Plp-Cre<sup>ERT</sup>;Mek1DD-eGFP/+* or *Pdgfra-Cre<sup>ERT</sup>;Mek1DD-eGFP* mice revealed this was not solely due to a protective or reparative effect resulting from MEK1DD expression specifically in the OL lineage. Because EAE is an immune-mediated disease, we examined *Cnp-Cre;Mek1DD-eGFP/+* splenic immune cells for recombination. Surprisingly, GFP<sup>+</sup> recombined CD19<sup>+</sup> B-cells, CD11b<sup>+</sup> monocytes, and CD3<sup>+</sup> T-cells were noted when Cre expression was driven by the *Cnp* promoter. While ERK1/2 signaling in monocytes and T-cells is associated with proinflammatory activation, fewer studies have examined ERK1/2 signaling in B-cell populations. After *in vitro* stimulation, MEK1DD-expressing B-cells exhibited a 3-fold increase in CD138<sup>+</sup> plasmablasts and a 5-fold increase in CD5<sup>+</sup>CD1d<sup>hi</sup> B-cells compared to controls. Stimulated MEK1DD-expressing B-cells also exhibited an upregulation of IL-10, known to suppress the initiation of EAE when produced by CD5<sup>+</sup>CD1d<sup>hi</sup> regulatory B-cells. Taken together, our data support the conclusion that sustained ERK1/2 activation in B-cells suppresses immune-mediated demyelination via increasing activation of regulatory B10 cells.

## Keywords

B10-cell, B-cell, demyelination, EAE, oligodendrocyte, ERK1/2

Received July 13, 2020; Revised September 29, 2020; Accepted for publication October 9, 2020

Myelination, once thought to be a passive insulation surrounding axons, is now known to play an active role in modulating central nervous system (CNS) function. In addition to optimizing conduction velocity, oligodendrocytes (OLs), the myelinating cells of the CNS, provide trophic and metabolic support to axons without which axons degenerate (Funfschilling et al., 2012; Simons & Nave, 2015; Meyer et al., 2018). In demyelinating diseases such as multiple sclerosis (MS), autoimmune-mediated loss of myelin and oligodendrocytes (OLs) in

<sup>1</sup>Department of Pharmacology, Physiology, and Neuroscience, Rutgers University New Jersey Medical School, Newark, United States

<sup>2</sup>Center for Neuroscience, University of Pittsburgh, Pittsburgh, Pennsylvania, United States

<sup>3</sup>Center for Cell Signaling, Rutgers University New Jersey Medical School, Newark, United States

<sup>4</sup>Department of Pediatrics, Division of Neurology, University of Pittsburgh, Pittsburgh, Pennsylvania, United States

Sharyl L. Fyffe-Maricich is presently affiliated with Ultragenyx Pharmaceutical, Novato, CA 94949, United States.

## Corresponding Authors:

Sharyl L. Fyffe-Maricich, Ultragenyx Pharmaceutical, 60 Leveroni Ct., Novato, CA 94949, United States.

Email: SFyffe-Maricich@ultragenyx.com

Teresa L. Wood, Rutgers New Jersey Medical School, 205 S. Orange Ave., Cancer Center H1200, Newark, NJ 07103, United States.

Email: terri.wood@rutgers.edu



the central nervous system (CNS) results in damage to neurons causing a progressive decline in patient mobility. Current immunosuppression treatments do not adequately prevent demyelination and disease progression. Additionally, no therapeutic options exist that target OLs to increase resistance to immune attack or promote myelin repair. Therefore, additional research to elucidate mechanisms of limiting demyelination and stimulating remyelination is critical to increase therapeutic efficacy.

Previous studies have examined the role of extracellular signal-regulated kinases 1 and 2 (ERK1/2) in developmental myelination and remyelination (Ishii et al., 2012; Fyffe-Maricich et al., 2013; Ishii et al., 2013; Michel et al., 2015; Jeffries et al., 2016). Of particular importance are data revealing that ERK1/2 signaling critically promotes timely myelin repair and can regulate remyelination thickness after lysophosphatidylcholine (LPC) injection, a detergent that disrupts lipid-rich myelin membranes leading to focal demyelination. When ERK2 is conditionally deleted in the OL lineage, this results in delayed myelin wrapping after LPC demyelination of the corpus callosum (Michel et al., 2015). Conversely, sustained ERK1/2 activation in the OL lineage leads to enhanced myelin thickness during remyelination after LPC injection into the spinal cord without affecting demyelination (Fyffe-Maricich et al., 2013). Surprisingly, sustained ERK1/2 activation specifically in mature OLs prior to demyelination results in MEK1DD-expressing pre-existing OLs that persist in a LPC lesion and form myelin basic protein (MBP) positive processes that may contribute to remyelination, which normally does not occur (Jeffries et al., 2016). Taken together, these studies have highlighted ERK1/2 signaling in the OL lineage as a key regulator of remyelination, particularly with regards to myelin thickness. However, to date no studies have examined ERK1/2 signaling in the OL lineage in an immune-mediated model of demyelination like experimental autoimmune encephalomyelitis (EAE), which recapitulates the immune component of MS pathology.

In order to determine whether sustained ERK1/2 activation in the OL lineage results in decreased EAE severity, we examined *Cnp-Cre;Mek1DD-eGFP/+* (Cnp-Mek1DD) mice that express constitutively-active MEK1, the upstream kinase of ERK1/2, under the *Cnp* promoter which drives expression in the OL lineage in the CNS and Schwann cells in the peripheral nervous system (PNS). Previous studies using this mouse line have revealed hypermyelination throughout the CNS and PNS (Fyffe-Maricich et al., 2013; Ishii et al., 2013). In particular, Cnp-Mek1DD mice exhibited increased remyelination thickness after LPC demyelination of the spinal cord (Fyffe-Maricich et al., 2013). Because these mice exhibit hypermyelination during myelin repair after LPC injection, we hypothesized that we might similarly

see a beneficial effect of ERK1/2 signaling in the context of EAE. Extraordinarily, we found that Cnp-Mek1DD mice did not develop severe EAE symptoms like their control littermates, suggesting a protective effect against EAE induction. To validate these results we used a tamoxifen-inducible Cre-lox mouse model, *Plp-Cre<sup>ERT</sup>;Mek1DD-eGFP/+* (Plp-Mek1DD) that expresses MEK1DD in mature OLs only after exposure to tamoxifen. Plp-Mek1DD mice that were given tamoxifen 40 days prior to EAE induction exhibited a disease course similar to control mice, indicating that sustained ERK1/2 activation in mature OLs, and the accompanying increased myelin thickness, does not protect against EAE. In order to examine whether Cnp-Mek1DD mice had attenuated EAE disease course due to recombined oligodendrocyte progenitor cells (OPCs) responsible for remyelination, we administered tamoxifen to *Pdgfra-Cre<sup>ERT</sup>;Mek1DD-eGFP* (Pdgfra-Mek1DD) mice during EAE. However, these mice did not exhibit improved functional scores during EAE compared to controls, suggesting that sustained ERK1/2 activation in adult OPCs during remyelination does not improve function in the EAE model. Upon further examination, we discovered that the *Cnp* promoter was inducing recombination in splenic immune cell populations; namely, CD19<sup>+</sup> B-cells, CD11b<sup>+</sup> monocytes, and CD3<sup>+</sup> T-cells. Isolation of CD19<sup>+</sup> splenic B-cells from Cnp-Mek1DD and control mice followed by *in vitro* stimulation with lipopolysaccharides (LPS) resulted in enhanced B-cell activation. In particular, enriched expansion of the CD5<sup>+</sup>CD1d<sup>hi</sup> population and increased IL-10 transcription and secretion, associated with regulatory B10 cells, was observed. Taken together, our data reveal that the *Cnp* promoter is active not only in the OL lineage of the CNS, but also in splenic B-cells, monocytes, and T-cells. Furthermore, expression of constitutively active MEK1 in splenic B-cells results in increased activation, particularly for IL-10 producing regulatory B10 cells. The results from this study suggest that enhancing B10 cell activation and function through downstream effectors of ERK1/2 signaling may be of therapeutic interest in preventing progressive damage in immune-mediated demyelination disorders such as MS.

## Materials and Methods

### Experimental Animals

Heterozygous *Cnp-Cre* (Lappe-Siefke et al., 2003), *Plp-Cre<sup>ERT</sup>* (Doerflinger et al., 2003) (The Jackson Laboratory, RRID:ISMR\_JAX:005975), or *Pdgfra-Cre<sup>ERT</sup>* (Kang et al., 2010) (The Jackson Laboratory, RRID:ISMR\_JAX:018280) mice on a C57Bl/6 background were bred to homozygous *R26Stop<sup>FL</sup>Mek1DD-eGFP* mice (Srinivasan et al., 2009) (The Jackson

Laboratory; RRID:ISMR\_JAX:012352) in order to generate female *Cnp-Cre;Mek1DD-eGFP/+* (*Cnp-Mek1DD*), *Plp-Cre<sup>ERT</sup>;Mek1DD-eGFP/+* (*Plp-Mek1DD*), or *Pdgfr $\alpha$ -Cre<sup>ERT</sup>;Mek1DD-eGFP/+* (*Pdgfr $\alpha$ -Mek1DD*) mice and control littermates (*WT;Mek1DD-eGFP/+*). In the *Cnp-Mek1DD* mouse CNS, the OL lineage exhibits recombination and expression of MEK1DD, a constitutively active MEK1 mutant rat MAPKK1 (the ERK1/2 kinase) with two serine to aspartic acid substitutions (S218D/S222D) within the catalytic domain. For some experiments, *Cnp-Cre* or *Plp-Cre<sup>ERT</sup>* mice were crossed with *ROSA<sup>mT/mG</sup>* double reporter (DR) (Muzumdar et al., 2007) (The Jackson Laboratory; RRID:ISMR\_JAX:007676) mice to generate *Cnp-Cre; ROSA<sup>mT/mG</sup>* (*Cnp-DR*) or *Plp-Cre<sup>ERT</sup>; ROSA<sup>mT/mG</sup>* (*Plp-DR*) mice that exhibit widespread membrane-bound TdTomato expression but upon Cre recombination express membrane-bound GFP in recombined cells. In order to induce recombination in *Plp-Mek1DD*, *Plp-DR*, or *Pdgfr $\alpha$ -Mek1DD* mice, tamoxifen (100 mg/kg; 10 mg/mL stock in 9:1 sunflower seed oil:ethanol) was administered by intraperitoneal injection for 5 consecutive days, resulting in the recombination in PLP<sup>+</sup> mature OLs or PDGFR $\alpha$ <sup>+</sup> OPCs respectively. In *Cnp-Mek1DD* and *Plp-Mek1DD* mice, expression of MEK1DD is concurrent with an eGFP marker downstream of an internal ribosomal entry site, such that recombined cells can be identified. Mice were kept in microisolation in a pathogen-free environment and maintained on a 12h light:12 h dark cycle with standard mouse chow and water *ad libitum*. All research and animal care procedures were approved by the University of Pittsburgh Institutional Animal Care and Use Committee or the Rutgers New Jersey Medical School Institutional Animal Care and Use Committee.

### Experimental Autoimmune Encephalomyelitis

In order to induce immune-mediated demyelination of the CNS in *Cnp-Mek1DD* and control littermates, 10-14 week old female mice were given EAE according to the MOG<sub>35-55</sub> peptide EAE kit (EK-2110, Hooke Laboratories). To induce recombination before EAE, 6-11 week old *Plp-Mek1DD* and control female mice were administered tamoxifen (10 mg/mL; T5648, Sigma) dissolved in 9:1 sunflower seed oil and ethanol by intraperitoneal injection at 100 mg/kg once daily for 5 consecutive days. The first injection was given 40 days prior to EAE induction at 12-17 weeks of age in order to allow for significant hypermyelination, observed previously by 21-60 days post-tamoxifen (dpt) (Jeffries et al., 2016). *Pdgfr $\alpha$ -Mek1DD* and control littermate mice were given EAE at 10-12 weeks of age. Each mouse received tamoxifen injections as described above once daily for 5 consecutive days once a clinical score of 1 was reached.

When mice reached a paralyzed state during EAE, they received softened wet mouse chow *ad libitum* and were checked daily for signs of dehydration and weight loss. If mice exhibited dehydration, they were administered 500  $\mu$ L of 0.9% saline subcutaneously once daily. Only female mice were used in all experiments as EAE induction in males results in higher unpredictability and variability in disease.

### Luxol Fast Blue Staining of Frozen Sections

Mice were intracardially perfused with 1 $\times$  PBS followed by 4% PFA/PBS, post-fixed for 2–24 hours, then cryo-protected overnight in 20% sucrose. Fixed spinal cord tissue was embedded and cryosectioned at 20  $\mu$ m sections. Sections were then rinsed in water followed by 35% and 70% EtOH, then incubated in luxol fast blue solution overnight at 55-60°C. Excess stain was rinsed with 95% EtOH followed by water, then destaining was performed in 0.05% lithium carbonate solution before additional 70% and 100% EtOH rinsing followed by xylene immersion and coverslipping.

### Immunolabeling of Frozen Sections

Mice were intracardially perfused with 1 $\times$  PBS followed by 4% PFA/PBS, post-fixed for 2-24 hours, then cryo-protected overnight in 20% sucrose. Fixed spinal cord tissue was embedded and cryosectioned at 20  $\mu$ m sections. Immunolabeling was performed as described previously in (Jeffries et al., 2016) with slight modifications. Briefly, for MBP immunofluorescence, sections were rehydrated in 1 $\times$  PBS then submerged in 100% EtOH for 10 minutes (min). After 3 washes in 1 $\times$  PBS, sections were blocked in 2-4% NGS/0.3% Triton-X-100 in 1 $\times$  PBS, then incubated with primary antibodies diluted in blocking buffer at 4°C overnight. After primary antibody incubation, sections were washed 3x 5 min. in 1 $\times$  PBS followed by secondary antibodies at room temperature for 1-3 hours. Primary antibodies used were mouse anti-MBP (1:1000; SMI-99, Covance, RRID:AB\_2314772), rabbit anti-IBA1 (1:500; 019-19741, Wako, RRID:AB\_839504), rat anti-CD3 (1:50; MAB4841, R&D Systems, RRID:AB\_358426), and rabbit anti-CD19 (1:1000; 90176, Cell Signaling, RRID:AB\_2800152). Secondary antibodies used were goat anti-mouse 488 (1:500; A11001, Invitrogen, RRID:AB\_2534069), goat anti-rabbit 546 (1:500; A11010, Invitrogen, RRID:2534077), goat anti-rat 350 (1:500; A21093, Invitrogen, RRID:AB\_2535748), goat anti-rabbit 647 (1:500; A21246, Invitrogen, RRID:AB\_2535814). Sections were counterstained with DAPI (1:1000) in order to identify demyelinated lesions by hypercellularity. Slides were coverslipped with Fluorogel (17985-10,

Electron Microscopy Sciences) or Prolong Gold (P36934, ThermoFisher Scientific).

### Toluidine Blue Sections

Mice were intracardially perfused with 4% PFA, then spinal cords were dissected and drop-fixed in 4% PFA/2% glutaraldehyde in 0.1 M sodium cacodylate buffer for  $\geq 24$  hrs. Tissue samples were postfixed in 1% OsO<sub>4</sub>, then dehydrated in serial ethanol solutions, stained *en bloc* with uranyl acetate, and embedded in a Poly/Bed812 resin. Thick (350 nm) sections were cut and stained with toluidine blue and visualized at 60x magnification.

### Image Analysis

Fluorescence and brightfield images were acquired using an Olympus AX-70 microscope and iVision software. Immunofluorescence images for analysis were acquired using a 2x objective. Toluidine blue ventral spinal cord white matter sections were imaged using a 60x oil objective. Imaged areas were selected for sparse or no visible immune infiltration and demyelination. Luxol fast blue images were acquired using a 2x objective. CD3 and CD19 immunostaining images were acquired using a 10x objective. For MBP and IBA1 positivity in the white matter of the spinal cord, the dorsal and ventral white matter regions were outlined as the region of interest (ROI). Images for analyzed using the adjust threshold function for positive staining and area fraction within the ROI was calculated using ImageJ software. At least 2 images per animal and 3 animals per genotype were analyzed.

### Spleen Dissociation

Female Cnp-Mek1DD, Cnp-DR, or Plp-DR and control littermate mice were euthanized by CO<sub>2</sub> inhalation at 8-13 weeks of age. Spleens were removed and immediately placed in 2 mL DMEM on ice, and dissociated as described previously with modifications (Pachynski et al., 2015). Spleens were chopped and 1 mL of digestion medium in HBSS added (0.04 mg/mL collagenase I, LS004214, Worthington Biochemical; 1.67 mg/mL collagenase IV, LS004188, Worthington Biochemical; 30 mg/mL DNase I, D4527-40KU, Sigma) for 25 min. incubation at 37°C, then 5 mL of DMEM were added and suspension filtered through a 70  $\mu$ m filter. Cells were centrifuged at 450 g for 6 min., then erythrocytes were lysed using 8.29 g/L NH<sub>4</sub>Cl, 1 g/L KHCO<sub>3</sub>, and 37.2 mg/L EDTA for 4 min. After adding 12 mL of DMEM, suspensions were filtered through a 70  $\mu$ m filter, washed with 10 mL DMEM, and centrifuged at 450 g for 6 min. Cells were resuspended in 20 mL of HBSS, centrifuged at 450 g for 5 min., then resuspended in 1 mL HBSS for cell counting with trypan blue. After

cell counting with a 1:4 dilution, cells were centrifuged at 450 g for 5 min. and resuspended at  $1 \times 10^6$  cells/50  $\mu$ L of FACS buffer (2% goat serum, G9023, Sigma; 1% BSA, A6003, Sigma; in HBSS). Only female mice were used for all immune cell experiments in order to match EAE experiments.

### Splenic Flow Cytometry

Resuspended splenic immune cells in FACS buffer were immunostained using appropriate combinations of the following antibodies in 50  $\mu$ L FACS buffer/sample: anti-CD45-PE/Cy5 (103109, RRID:AB\_312974), anti-CD19-PE/Cy7 (115520, RRID:AB\_313655), anti-CD3-BV510 (100233, RRID:AB\_2561387), anti-CD4-APC (100411, RRID:AB\_312696), anti-CD8a-PE (100707, RRID:AB\_312746), anti-CD11b-BV605 (101237, RRID:AB\_11126744), anti-MHCII-APC/Cy7 (107627, RRID:AB\_1659252), anti-CD5-PE/Cy5 (100609, RRID:AB\_312738), anti-CD1d-PE (123509, RRID:AB\_1236547), anti-CD138-BV510 (142521, RRID:AB\_2562727). All antibodies were obtained from BioLegend (San Diego, CA). Cells were incubated in primary antibodies for 40 min. in the dark, followed by the addition of 50  $\mu$ L of heat-inactivated FBS (F0926, Sigma) and centrifugation. For GFP+ recombination experiments, PacBlue Live/Dead staining (L34955, Invitrogen) was performed to verify viability in addition to trypan blue cell counts prior to staining to assess viability. For all analyses, cells were fixed with 1% PFA (15714-S, Electron Microscopy Sciences) for 7 min., centrifuged at 600 rcf, washed with  $1 \times$  PBS, and resuspended in 700  $\mu$ L of  $1 \times$  PBS for flow cytometry. Compensation was performed with unstained control cells, GFP+ Cnp-Mek1DD cells, and control cell samples individually stained with each antibody prior to all analyses with a BD LSRFortessa X-20 equipped with 5 lasers (355 nm, 405 nm, 488 nm, 561 nm, and 642 nm). 10000-50000 events were recorded for all analyses. Gating analysis was performed using FlowJo software.

### Flow Sorting

After spleen dissociation as described above, splenic immune cells were resuspended at  $20 \times 10^6$  cells/mL in FACS buffer. Immunostaining using anti-CD19-PE/Cy7 was performed at a concentration of 0.2  $\mu$ g/mL in 2 mL total volume. After a 40 min. incubation in primary antibody, 1 mL of heat-inactivated FBS (F0926, Sigma) was added to each sample before centrifugation at 450 rcf for 6 min. Cells were counterstained with DAPI for 15 min. to exclude dead cells (1:10000). After centrifugation at 450 rcf for 6 min., cells were resuspended in 1 mL of FACS buffer for flow sorting. Live CD19<sup>+</sup> B-cells were isolated for *in vitro* experiments using a BD FACSAria II

SORP. In control samples the CD19<sup>+</sup> population was collected, while in Cnp-Mek1DD samples the CD19<sup>+</sup>GFP<sup>+</sup> population was collected. Cells were sorted into B-cell collection media containing 10% heat-inactivated FBS (F0926, Sigma), 2 mM l-glutamine, 50  $\mu$ M 2-mercaptoethanol (21985023, Thermofisher Scientific), 1 mM sodium pyruvate (11360-070, Gibco), 10 mM HEPES (15630-080, Gibco), and 1 $\times$  pen-strep in RPMI-1640.

### B-Cell Culture

Flow-sorted CD19<sup>+</sup> B-cells were centrifuged at 450 g then resuspended in 1 mL B-cell collection media (described above). Viable B-cells were counted using trypan blue to exclude dead cells. Samples were then centrifuged and resuspended at 2  $\times$  10<sup>6</sup>/mL in B-cell culture media containing 10% heat-inactivated FBS (Lot# 15C487, F0926, Sigma), 2 mM l-glutamine, 50  $\mu$ M 2-mercaptoethanol (21985023, Thermofisher Scientific), 1 mM sodium pyruvate (11360-070, Gibco), 1 $\times$  pen-strep, and 10  $\mu$ g/mL lipopolysaccharides (LPS; L2630, Sigma) in RPMI-1640. B-cells were plated in 96-well TSS plates at 2  $\times$  10<sup>5</sup>/well (200  $\mu$ L/well) and cultured at 37°C for 48 hrs. To examine the production of IL-10 specifically, additional stimulation was performed with PMA (50 ng/mL; P1585, Sigma) and ionomycin (500 ng/mL; I9657, Sigma) for the last 5 hrs. of culture (Yanaba et al., 2008).

### Quantitative Reverse Transcription Polymerase Chain Reaction

Stimulated B-cells were collected from individual wells on 96-well plates and centrifuged at 450 g for 5 min. Supernatant was removed and cells resuspended in 350  $\mu$ L of RLT buffer from the Qiagen RNeasy Mini Prep kit (74104, Qiagen), then frozen at -80°C for a minimum of 24 hrs. before additional processing. After thawing on ice, samples were prepared with the QiaShredder columns (79656, Qiagen) for homogenization followed by isolation with the Qiagen RNA Mini Prep kit. RNA concentration and quality was quantified using the Nanodrop and 156 ng of RNA was used for each cDNA reaction using Superscript II (18064014, Invitrogen). For quantitative reverse transcription polymerase chain reaction (qRT-PCR), 1.5  $\mu$ L of cDNA was used in each reaction with iTaq Universal SYBR Green Supermix (1725124, BioRad). Primers used were as follows: GAPDH Fwd: 5'-GATGCCCCCATGTTTG TGAT-3', GAPDH Rev: 5'GGTCATGAGCCCTTCC ACAAT-3', IL-10 Fwd: 5'-CAGCCGGGAAGACAAT AACT-3', IL-10 Rev: 5'-GTTGTCCAGCTGGTC CTTTG-3'.

### Enzyme-Linked Immunosorbent Assay

Conditioned media was collected from stimulated B cells cultured on a 96-well plate and centrifuged for 5 min at 1500 rpm to remove debris. The media was incubated with the mouse IL-10 Quantikine ELISA kit (M1000B, R&D Systems) according to manufacturer's protocol. Levels of IL-10 were detected using the Gene5 plate reader (BioTek) at an absorbance of 450 nm.

### Statistical Analysis

For experiments comparing two groups, Student's t test was used. When comparing two groups with multiple measurements, as for EAE scoring over time, two-way repeated measures ANOVA followed by Sidak's multiple comparisons test was used. F and p statistics for 2-way repeated measures ANOVA are reported in relevant figure legends, and statistical significance in graphs is represented using p value results from Sidak's multiple comparisons test. Sample sizes and p values are reported in each figure legend. All graphical data is represented as mean  $\pm$  SEM. For all experiments, \*\*\*\*p  $\leq$  0.0001, \*\*\*p  $\leq$  0.001, \*\*p  $\leq$  0.01, and \*p  $\leq$  0.05 unless otherwise stated.

## Results

### Cnp-Cre;Mek1DD/+ Mice Exhibit Improved EAE Clinical Score

Mice with sustained activation of ERK1/2 in the OL lineage exhibit hypermyelination throughout the CNS, and thicker remyelination in a focal LPC-induced demyelinated lesion of the spinal cord (Fyffe-Maricich et al., 2013; Ishii et al., 2013). While previous studies used the LPC model of demyelination to examine loss and repair of myelin in the CNS, we wanted to determine whether sustained ERK1/2 activation in the OL lineage is beneficial in an immune-mediated demyelination model similar to MS. Therefore, we induced MOG<sub>35-55</sub> EAE in female Cnp-Mek1DD and control littermate mice at 10-14 weeks of age (Figure 1A). EAE clinical severity was assessed daily starting at 7 days post-induction (dpi) using the standard scoring protocol, with normal locomotion scored as 0 and moribund scored as 5. Cnp-Mek1DD mice exhibited a significantly reduced score versus control littermates from 13 dpi until the end of scoring at 24 dpi, nearly the entire disease course (Figure 1B; \*p = 0.01, \*\*p = 0.002 - 0.008, \*\*\*p = 0.0002 - 0.0005, \*\*\*\*p < 0.0001). Upon further examination, both peak score (Control = 3.7, Cnp-Mek1DD = 2.3; p = 0.004) and maximum improvement (Control = 0.4, Cnp-Mek1DD = 1.1; p = 0.02) were also significantly improved, while control animals exhibited a standard

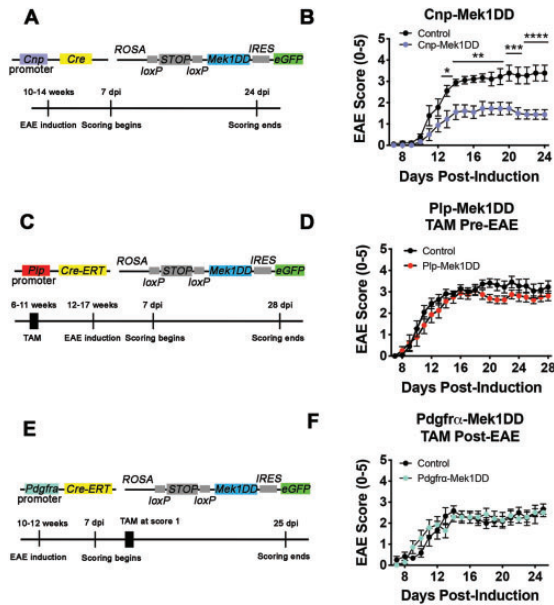


**Figure 1.** Cnp-Mek1DD Mice Display Reduced EAE Clinical Score Compared to Controls. A: Schematic diagram showing constructs for Cnp-Mek1DD mouse and the EAE induction paradigm used. B: EAE clinical scores from Cnp-Mek1DD (blue) and control (black) mice,  $n = 9/\text{group}$ . Two-way repeated measures ANOVA was significant ( $F(17,272) = 4.876$ ;  $p < 0.0001$ ). Significance depicted based on Sidak's multiple comparisons test after two-way ANOVA. C: Schematic diagram showing constructs for Plp-Mek1DD mouse and the EAE induction paradigm used, with tamoxifen (TAM) injections prior to EAE induction. D: EAE clinical scores from control (black) and Plp-Mek1DD (red) mice given TAM prior to EAE induction,  $n = 8-11/\text{group}$ . Two way repeated measures ANOVA was not significant ( $F(21,357) = 0.75$ ;  $p = 0.78$ ). E: Schematic diagram showing constructs for Pdgfra-Mek1DD mouse and the EAE induction paradigm used, with tamoxifen (TAM) injections given at score  $\geq 1$  for each mouse. F: EAE clinical scores from control (black) and Pdgfra-Mek1DD (green) mice given TAM during EAE disease,  $n = 6-7/\text{group}$ . Two-way repeated measures ANOVA was not significant ( $F(18,198) = 1.21$ ;  $p = 0.25$ ). All graphical data are presented as mean  $\pm$  SEM. \* $p \leq 0.05$ , \*\* $p \leq 0.01$ , \*\*\* $p \leq 0.001$ , \*\*\*\* $p \leq 0.0001$ .

chronic MOG<sub>35-55</sub> disease course for C57Bl/6 mice (Rangachari & Kuchroo, 2013; Terry et al., 2016). To validate the observed protective effect in Cnp-Mek1DD mice, we used tamoxifen inducible *Plp-Cre<sup>ERT</sup>;Mek1DD-eGFP/+* (Plp-Mek1DD) and CRE-negative control littermate mice, which exhibit recombination in PLP<sup>+</sup> mature OLs at the time of tamoxifen injection (Ishii et al., 2016; Jeffries et al., 2016). In order to determine whether ERK1/2-induced hypermyelination was protective against the development or severity of ascending hind-limb paralysis caused by EAE-induced demyelination, we administered tamoxifen to 6-11 week old female Plp-Mek1DD and control littermate mice 40 days before inducing EAE (Figure 1C). Previous work has demonstrated that significant hypermyelination is observed in

Plp-Mek1DD mice between 21-60 days post tamoxifen (dpt) (Jeffries et al., 2016). EAE induction at 12-17 weeks of age resulted in comparable disease initiation, as measured by the timing of onset of clinical symptoms in both Plp-Mek1DD and control mice. Moreover, there were no significant differences in EAE clinical scores throughout the 28 days following EAE induction, suggesting that hypermyelination driven by ERK1/2 activation is not protective against EAE induction or the severity of the clinical signs that develop (Figure 1D;  $p = 0.71 - 0.99+$ ). *Cnp-Cre* additionally causes *loxP*-mediated recombination in OPCs that give rise to newly-generated mature OLs responsible for remyelination. To address whether MEK1DD expression in OPCs results in improved functional score in the EAE model, we induced EAE in 10-12 week old female *Pdgfra-Cre<sup>ERT</sup>;Mek1DD-eGFP/+* (Pdgfra-Mek1DD) and control littermate mice. Upon exhibiting an EAE clinical score of 1 or greater, each mouse was given tamoxifen for five consecutive days to induce recombination in OPCs (Figure 1E). However, this did not result in any change in EAE disease course in Pdgfra-Mek1DD mice compared to controls, suggesting that sustained ERK1/2 activity in OPCs does not improve functional score in EAE during remyelination (Figure 1F;  $p = 0.83 - 0.99+$ ).

Toluidine blue staining in spinal cord ventral white matter revealed that both Cnp-Mek1DD and Plp-Mek1DD mice displayed visible hypermyelination compared to controls at the end of EAE disease course comparable in magnitude to previously published observations (Figure 2A and B) (Ishii et al., 2013; Jeffries et al., 2016). Luxol fast blue staining showed extensive lesions throughout the white matter of the control spinal cord at the end of EAE disease course, while no lesions were visible in the Cnp-Mek1DD spinal cord (Figure 2C). In order to further investigate changes in Cnp-Mek1DD EAE spinal cords compared to controls, we immunostained for myelin basic protein (MBP) at 24 dpi. MBP staining revealed widespread areas lacking MBP in control spinal cords. Areas with reduced MBP staining were also apparent in the white matter of the spinal cord of Cnp-Mek1DD mice, however, these were small and sparsely distributed (Figure 2D). We found that the percentage of white matter that lacked MBP expression was significantly decreased in the ventral white matter of Cnp-Mek1DD mice (Figure 2D and E; Control = 28.61%, Cnp-Mek1DD = 13.66%;  $p = 0.0006$ ) but not in the dorsal white matter when quantifying MBP<sup>-</sup> area (Figure 2D and E; Control = 21.97%, Cnp-Mek1DD = 19.77%;  $p = 0.71$ ). Despite this, we observed that the ventral white matter displayed unchanged IBA1<sup>+</sup> area (Figure 3A and B; Control = 43.63%, Cnp-Mek1DD = 30.49%;  $p = 0.32$ ), a marker for microglia and macrophages, while dorsal white matter IBA<sup>+</sup> was significantly decreased (Figure

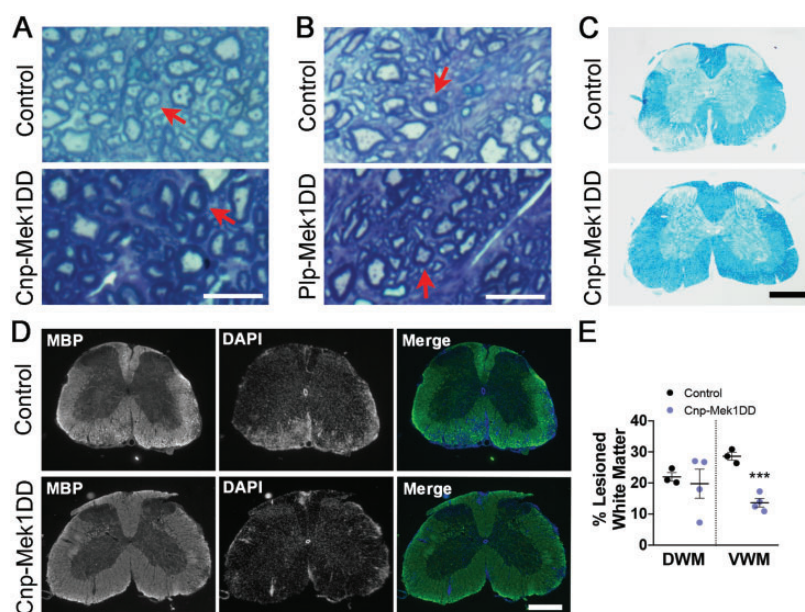


**Figure 2.** Cnp-Mek1DD Mice Display Hypermyelination and Reduced Lesion Load at the End of EAE Disease Course. A: Representative toluidine blue images from control and Cnp-Mek1DD spinal cord ventral white matter. Red arrows point to similarly sized axons. Scale bar = 10  $\mu$ m. B: Representative toluidine blue images from control and Plp-Mek1DD spinal cord ventral white matter. Red arrows point to similarly sized axons. Scale bar = 10  $\mu$ m. C: Luxol fast blue staining of control and Cnp-Mek1DD spinal cords at 24 dpi, scale bar = 500  $\mu$ m. D: Myelin basic protein (MBP, green) and DAPI (blue) immunostaining of control and Cnp-Mek1DD spinal cords at 24 dpi, scale bar = 500  $\mu$ m. E: The % of dorsal white matter (DWM) and ventral white matter (VWM) that is lesioned in control and Cnp-Mek1DD spinal cords, n = 3-4/group.

3A and B; Control = 36.92%, Cnp-Mek1DD = 11.27%;  $p = 0.008$ ). Finally, we immunostained control and Cnp-Mek1DD 24dpi spinal cords for CD3, a marker of T-cells, and CD19, a marker of B-cells (Figure 3C). In all three control animals, extensive lesions, identified by DAPI hypercellularity, were observed throughout the ventral and dorsal white matter (Figure 3C). In contrast, Cnp-Mek1DD mice displayed very few, small lesions identified by DAPI, with one animal exhibiting no apparent lesions at all using this method. Within these lesions, we could identify both CD3<sup>+</sup> T-cell infiltration and rare CD19<sup>+</sup> B-cell infiltration (Figure 3C). These images highlight the very low lesion load of Cnp-Mek1DD mice during EAE despite apparent activation of microglia/macrophages and infiltration of CD3<sup>+</sup> and CD19<sup>+</sup> cells within existing lesions.

While both Cnp-Mek1DD and Plp-Mek1DD mice displayed hypermyelination consistent with prior observations (Fyffe-Maricich et al., 2013; Ishii et al., 2013; Jeffries et al., 2016), only Cnp-Mek1DD mice developed an attenuated clinical course of EAE disease. Additionally, data from Pdgfra-Mek1DD mice demonstrated that MEK1DD expression in OPCs did not result in improved EAE disease course. Interestingly, while the loss of MBP was modest in the ventral white matter of Cnp-Mek1DD spinal cords compared to controls, an expansion of IBA1<sup>+</sup> area was comparable to controls,

and infiltration of CD3<sup>+</sup> T-cells and CD19<sup>+</sup> B-cells was occasionally observed.

### The Cnp Promoter Drives CRE Expression in Splenic Immune Cell Populations

Our data in Cnp-Mek1DD mice revealed significant improvement in EAE clinical score compared to controls, yet data using tamoxifen-inducible Plp-Mek1DD or Pdgfra-Mek1DD mice did not support the conclusion that MEK1DD expression in the OL lineage provides a protective or reparative functional benefit. These data were surprising, given that *Cnp-Cre* has previously been reported to cause recombination specifically in the OL lineage in the CNS (Nishizawa et al., 1985; Trapp et al., 1988; Lappe-Siefke et al., 2003; Madsen et al., 2016; Mei et al., 2016; Joseph et al., 2019; Y. Yue et al., 2019). However, there are reports of *Cnp* promoter activity in cell types outside of the CNS, including immune cell populations (Sheedlo et al., 1984; McFerran & Burgoyne, 1997; Miyoshi et al., 2001; Davidoff et al., 2002; F. Yue et al., 2014). Therefore, we hypothesized that *Cnp-Cre* was driving recombination to enable expression of MEK1DD in immune cells that mediate EAE. In order to determine whether this was the case, we examined immune cell populations from the spleens of 8-11 week old female Cnp-Mek1DD and

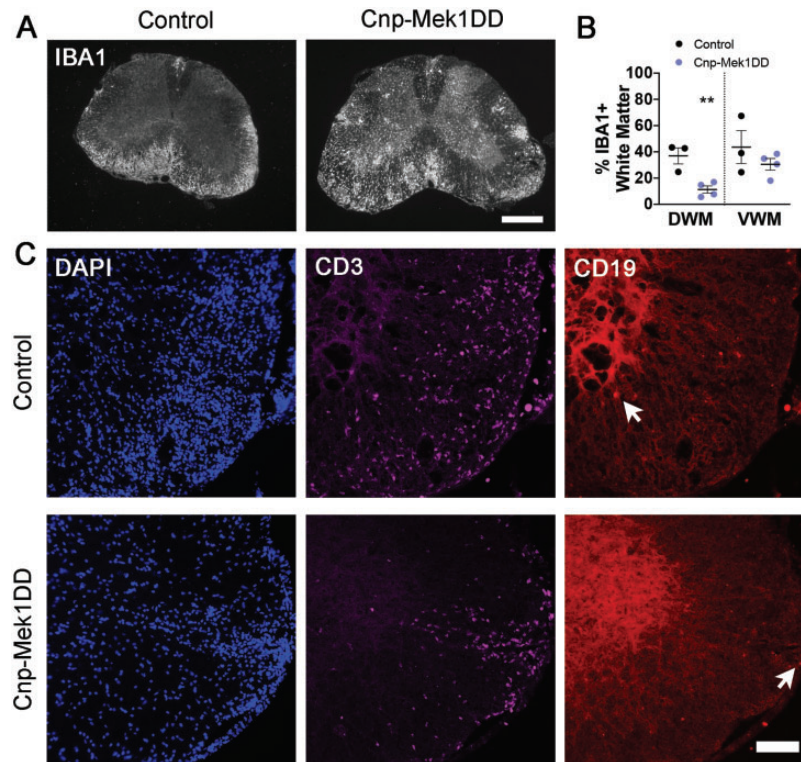


**Figure 3.** Cnp-Mek1DD Spinal Cords Exhibit Sparse Lesions With Evidence of Immune Cell Infiltration and Inflammation. A: IBA1 immunostaining of control and Cnp-Mek1DD spinal cords at 24 dpi, scale bar = 500  $\mu$ m. B: The % of dorsal white matter (DWM) and ventral white matter (VWM) that is positive for IBA1 in control and Cnp-Mek1DD spinal cords, n = 3-4/group. C: Representative images of DAPI (blue), CD3 (magenta), and CD19 (red) immunostaining in control and Cnp-Mek1DD lesions at 24 dpi, scale bar = 100  $\mu$ m. White arrows point to CD19<sup>+</sup> B-cells.

control littermate mice. To our surprise, we discovered that ~25-40% of live splenic cells were GFP<sup>+</sup> (data not shown) in Cnp-Mek1DD mice, while CRE-negative controls only exhibited 1-3% GFP<sup>+</sup> background. The absence of CRE but presence of the *R26Stop<sup>Fl</sup>Mek1DD-eGFP* transgene in controls supports the conclusion that the GFP<sup>+</sup> population is a result of CRE-mediated recombination of the transgene. Upon further gating analysis, we determined that ~50% of CD19<sup>+</sup> B-cells co-expressed GFP (Figure 4A and E; Control = 0.92%, Cnp-Mek1DD = 52.61%), ~30% of CD11b<sup>+</sup> monocytes co-expressed GFP (Figure 4B and E; Control = 7.58%, Cnp-Mek1DD = 29.18%), ~25% of CD3<sup>+</sup>CD4<sup>+</sup> T-cells co-expressed GFP (Figure 4C and E; Control = 1.20%, Cnp-Mek1DD = 24.56%), and ~30% of CD3<sup>+</sup>CD8<sup>+</sup> T-cells co-expressed GFP (Figure 4D and E; Control = 2.45%, Cnp-Mek1DD = 30.49%). In B-cell and T-cell populations, we observed GFP<sup>hi</sup> and GFP<sup>lo</sup> expressing clusters that were both identified as GFP<sup>+</sup> for analysis. Due to variability in the position of the GFP<sup>lo</sup> cluster in the CD19<sup>+</sup> B-cell population, in some samples the GFP<sup>lo</sup> group could not be included in the gate, resulting in two distinct trials exhibiting ~40% or ~70% recombination (Figure 4E). However,

based on the presence of GFP<sup>hi</sup> and GFP<sup>lo</sup> CD19<sup>+</sup> B-cells in all samples regardless of gating, we suggest that *Cnp-Cre* drives *loxP* recombination in ~70% of CD19<sup>+</sup> B-cells rather than ~50%. In addition, we examined GFP<sup>+</sup> splenic cells and found that ~80% of the GFP<sup>+</sup> cells were CD19<sup>+</sup> B-cells while ~20% of the GFP<sup>+</sup> cells were CD3<sup>+</sup> T-cells and only ~4% were CD11b<sup>+</sup> monocytes revealing that in the spleen, *Cnp-Cre* primarily drives *loxP* recombination in B-cells and T-cells (Figure 4F and G).

We next examined recombination using female *Cnp-Cre; ROSA<sup>mT/mG</sup>* (Cnp-DR) carrying a double reporter that results in expression of membrane-bound GFP in recombined cells. This enabled us to evaluate *Cnp-Cre* mediated recombination without the presence of the *R26Stop<sup>Fl</sup>Mek1DD-eGFP* transgene, which might shift splenic immune cell populations. Flow analysis for GFP, CD45, CD19, CD3, and CD11b revealed that nearly 90% of CD19<sup>+</sup> B-cells (Supplemental Figure 1A; Control = 0.81%, Cnp-DR = 88.43%), ~40% of CD11b<sup>+</sup> monocytes (Supplemental Figure 1B; Control = 1.40%, Cnp-DR = 42.80%), and ~50% of CD3<sup>+</sup> T-cells (Supplemental Figure 1C; Control = 0.55%, Cnp-DR = 49.10%) were recombined.



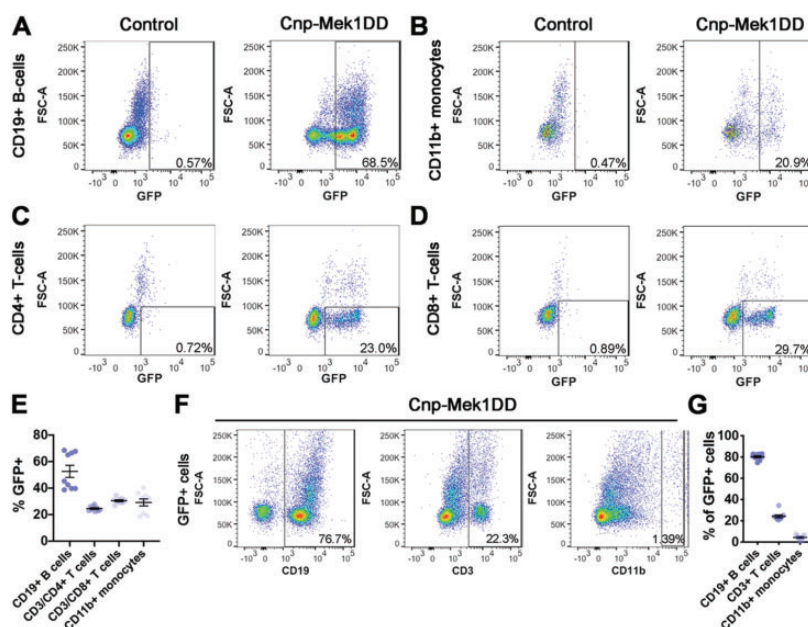


**Figure 4.** *Cnp-Mek1DD* Mice Display GFP<sup>+</sup> Recombined Splenic B-Cells, Monocytes, and T-cells. **A:** Representative flow cytometry dot plots from control and *Cnp-Mek1DD* splenic cells showing CD19<sup>+</sup> B-cells that are GFP<sup>+</sup>, n = 6-9/group. **B:** Representative flow cytometry dot plots from control and *Cnp-Mek1DD* splenic cells showing CD11b<sup>+</sup> monocytes that are GFP<sup>+</sup>, n = 6-9/group. **C:** Representative flow cytometry dot plots from control and *Cnp-Mek1DD* splenic cells showing CD3<sup>+</sup>CD4<sup>+</sup> T-cells that are GFP<sup>+</sup>, n = 6-9/group. **D:** Representative flow cytometry dot plots from control and *Cnp-Mek1DD* splenic cells showing CD3<sup>+</sup>CD8<sup>+</sup> T-cells that are GFP<sup>+</sup>, n = 6-9/group. **E:** Graph of the % of CD19<sup>+</sup>, CD3<sup>+</sup>CD4<sup>+</sup>, CD3<sup>+</sup>CD8<sup>+</sup>, and CD11b<sup>+</sup> cells that are GFP<sup>+</sup> in *Cnp-Mek1DD* spleens, n = 9. **F:** Representative flow cytometry dot plots from *Cnp-Mek1DD* splenic cells showing GFP<sup>+</sup> cells that are CD19<sup>+</sup>, CD11b<sup>+</sup>, or CD3<sup>+</sup>, n = 9. **G:** Graph of the % of GFP<sup>+</sup> cells that are CD19<sup>+</sup>, CD3<sup>+</sup>, or CD11b<sup>+</sup> in *Cnp-Mek1DD* spleens, n = 9.

The proportionally higher recombination rates may suggest that the stronger membrane-bound GFP reporter expressed by *Cnp-DR* mice identifies additional recombined cells that the fainter cytoplasmic GFP reporter expressed by *Cnp-Mek1DD* mice does not. Importantly, these data further demonstrate that *Cnp-Cre* drives recombination in splenic immune cell populations, particularly in CD19<sup>+</sup> B-cells.

In order to confirm that CRE-mediated recombination in splenic immune populations occurs under control of the *Cnp* promoter and not the *Plp* promoter, we conducted flow cytometry for GFP, CD45, CD19, CD3, and CD11b on *Plp-DR* mice. Female *Plp-DR* and control littermate mice without *Plp-Cre<sup>ERT</sup>* were administered tamoxifen to induce recombination at 11 weeks of age, and spleens collected 2 weeks after the first tamoxifen injection for analysis. Importantly, we did not observe any GFP<sup>+</sup> populations in the spleen when gating for CD19<sup>+</sup> B-cells, CD11b<sup>+</sup> monocytes, or CD3<sup>+</sup> T-cells (Figure 5A to C). The absence of GFP<sup>+</sup> splenic immune populations in *Plp-DR* mice supports our conclusion that the *Cnp* promoter drives the expression of CRE resulting in recombination in splenic immune cell populations, while other promoters that drive expression in the OL-lineage such as *Plp* do not. Taken together, these data suggest that in addition to the OL lineage, the

*Cnp* promoter drives CRE expression in splenic B-cells, T-cells, and monocytes, immune cell populations known to regulate EAE and other autoimmune diseases.

### Constitutively Active MEK1 Expression Increases In Vitro Activation of Splenic CD19<sup>+</sup> B-Cells

MOG<sub>35-55</sub> EAE was originally thought to be a T-cell mediated disease independent of B-cell function (Mendel et al., 1995; Lyons et al., 1999; Jager et al., 2009). However, recent studies and the clinical success of B-cell targeted drugs such as rituximab have revealed important roles for B-cell populations in EAE and MS (Mann et al., 2012; Pierson et al., 2014; Ray & Basu, 2014; Parker Harp et al., 2015; Hausser-Kinzel & Weber, 2019; Pennati et al., 2020). While GFP<sup>+</sup> recombined B-cells, T-cells, and monocytes were observed, recombination was higher in CD19<sup>+</sup> B-cells than T-cells or monocytes (Figure 2A to E), and the majority of GFP<sup>+</sup> cells were CD19<sup>+</sup> (Figure 2F and G). Additionally, limited research has been done to determine the role of ERK1/2 signaling in the function of specific B-cell populations. We first wanted to determine whether expression of MEK1DD resulted in baseline splenic B-cell population changes. In order to address this, we labeled splenic cells for CD19, CD1d, CD5,

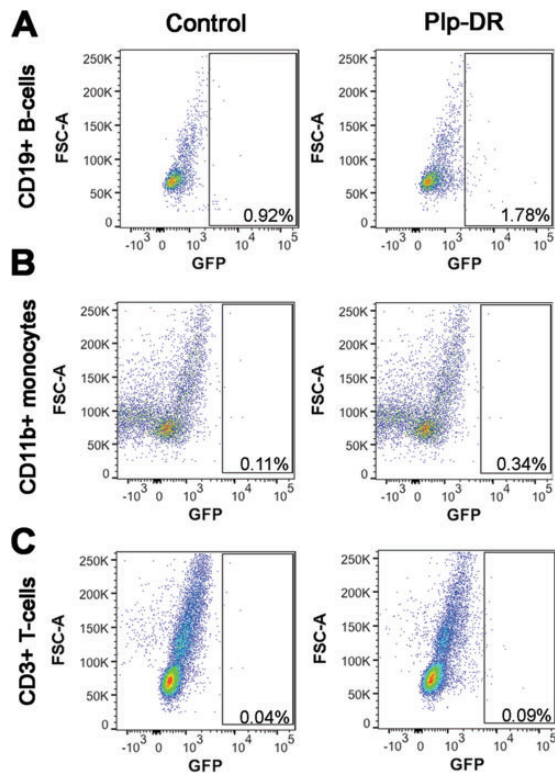


**Figure 5.** PIp-Cre<sup>ERT</sup> Does Not Drive Recombination in Splenic Immune Cells. A: Representative flow cytometry dot plots from control and PIp-DR splenic cells showing CD19<sup>+</sup> B-cells that are GFP<sup>+</sup>, n = 3/group. B: Representative flow cytometry dot plots from control and PIp-DR splenic cells showing CD11b<sup>+</sup> monocytes that are GFP<sup>+</sup>, n = 3/group. C: Representative flow cytometry dot plots from control and PIp-DR splenic cells showing CD3<sup>+</sup> T-cells that are GFP<sup>+</sup>, n = 3/group.

and CD138, each of which mark a defined subset of B-cells when combined with the CD19 pan-B-cell marker. The CD19<sup>+</sup>CD5<sup>+</sup>CD1d<sup>hi</sup> B-cell population is associated with a regulatory B10 cell subset, which has previously been shown to suppress EAE disease severity (Matsushita et al., 2008; 2010). Conversely, the CD19<sup>+</sup>CD138<sup>+</sup> population marks plasmablasts, which eventually differentiate into antibody-producing CD19<sup>+</sup>CD138<sup>+</sup> plasma cells that can positively or negatively modulate EAE inflammation (Shen et al., 2014; Chen et al., 2016; Pollok et al., 2017; Fillatreau, 2019). We did not observe any significant differences in the percentages of CD19<sup>+</sup> B-cells in the spleen (Figure 6A and D; Control = 36.60%, Cnp-Mek1DD = 40.88%; p = 0.54), CD5<sup>+</sup>CD1d<sup>hi</sup> cells out of CD19<sup>+</sup> B-cells (Figure 6B and E; Control = 2.22%, Cnp-Mek1DD = 3.03%; p = 0.12), or CD138<sup>+</sup> cells out of CD19<sup>+</sup> B-cells (Figure 6C and E; Control = 9.86%, Cnp-Mek1DD = 12.2%; p = 0.07). However, it was of particular interest for us to examine how the expression of MEK1DD in CD19<sup>+</sup> splenic B-cells affects activation,

which could in turn influence EAE disease course. We labeled splenic cells from Cnp-Mek1DD and control mice for CD19, then flow sorted for either CD19<sup>+</sup> cells (in control) or CD19<sup>+</sup>GFP<sup>+</sup> cells (in Cnp-Mek1DD). Importantly, flow sorting confirmed a recombination rate of ~70% in CD19<sup>+</sup> B-cells, with 7 Cnp-Mek1DD samples exhibiting GFP positivity between 62% and 78.2%, with a mean of 72.3% (data not shown). CD19<sup>+</sup> cells from control and CD19<sup>+</sup>GFP<sup>+</sup> cells from Cnp-Mek1DD spleens were then cultured for 72 hrs. and stimulated with LPS in order to induce B-cell proliferation and activation. After 72 hrs. in culture, B-cells were labeled for CD19, MHC-II, CD5, CD1d, and CD138 and analyzed by flow cytometry. Flow analysis revealed that LPS activation resulted in successful activation of control CD19<sup>+</sup> B-cells, with a high-expressing MHC-II<sup>+</sup> group evident in both control and Cnp-Mek1DD samples (Figure 7A and D). The percentage of CD19<sup>+</sup> B-cells that labeled as MHC-II<sup>hi</sup> was unchanged between controls and Cnp-Mek1DD stimulated B-cells (Figure 7A and D; Control = 32.75%, Cnp-Mek1DD = 46.53%; p = 0.28). However, when examining the percentage of CD5<sup>+</sup>CD1d<sup>hi</sup> cells within the CD19<sup>+</sup> population, we observed a 5-fold significant increase in the numbers of Cnp-Mek1DD B-cells within this population compared to controls, a subset of which are regulatory B10 cells (Figure 7B and E; Control = 2.33%, Cnp-Mek1DD = 10.82%; p = 0.008). Additionally, we observed a 3-fold significant increase in the percentage of CD19<sup>+</sup> B-cells expressing CD138 compared to controls, suggesting increased differentiation of B-cells into plasmablasts (Figure 7C and E; Control = 7.22%, Cnp-Mek1DD = 19.87%; p = 0.003). Taken together, these data suggest that activated ERK1/2 in CD19<sup>+</sup> B-cells results in increased expansion of CD5<sup>+</sup>CD1d<sup>hi</sup> and CD138<sup>+</sup> B-cell subsets, both of which modulate EAE disease severity (Matsushita et al., 2008, 2010; Shen et al., 2014; Fillatreau, 2019).

### MEK1DD Expression in Splenic CD19<sup>+</sup> B-Cells Results in Upregulated IL-10 Expression

Cytokine release by immune cells significantly impacts the severity and progression of EAE disease. For example, the proinflammatory cytokine IL-6 is critical for the induction of EAE through the modulation of Th1, Th2, and Th17 cell activation and function (Samoilova et al., 1998; Okuda et al., 1999; Serada et al., 2008), while the anti-inflammatory cytokine IL-10 significantly reduces the severity of EAE disease (Bettelli et al., 1998; Xiao et al., 1998; Cua et al., 1999). Specifically, IL-10 production by regulatory B10 cells can suppress EAE disease initiation in a manner similar to clinical scores seen in Cnp-Mek1DD mice (Matsushita et al., 2010). We wanted to determine whether the significant increase in the

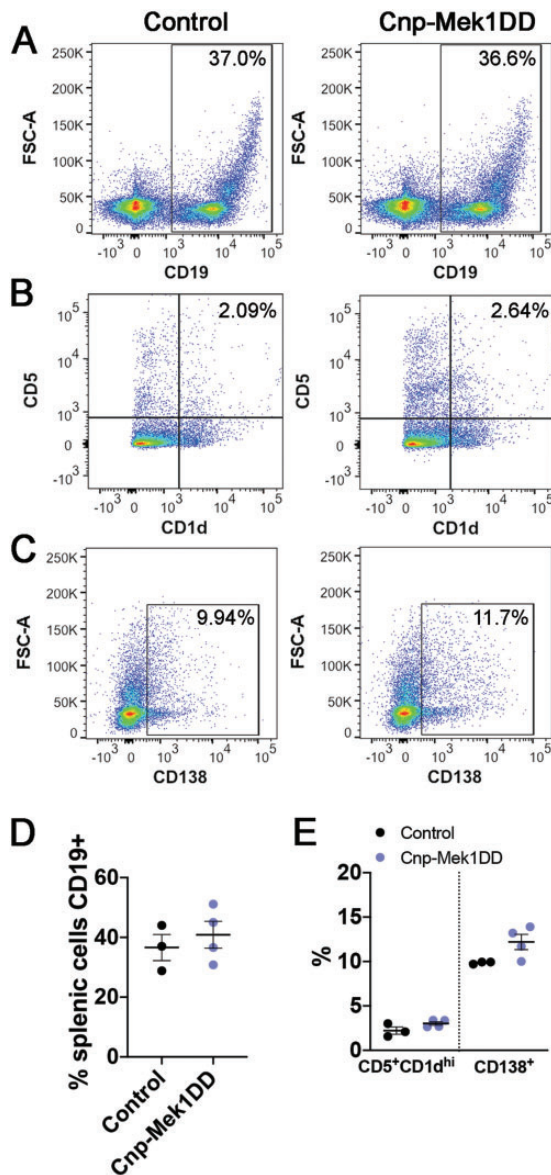


**Figure 6.** MEK1DD Expression in Splenic B-Cells Does Not Alter B-Cell Populations Pre-Stimulation. A: Representative flow cytometry dot plots from control and Cnp-Mek1DD splenic cells showing CD19<sup>+</sup> B-cells, n = 3-4/group. B: Representative flow cytometry dot plots from control and Cnp-Mek1DD splenic cells showing CD5<sup>+</sup>CD1d<sup>hi</sup> B-cells, n = 3-4/group. C: Representative flow cytometry dot plots from control and Cnp-Mek1DD splenic cells showing CD138<sup>+</sup> plasmablasts, n = 3-4/group. D: Graph showing % of control or Cnp-Mek1DD splenic cells expressing CD19, n = 3-4/group. E: Graph showing % of CD19<sup>+</sup> control or Cnp-Mek1DD splenic cells that are CD5<sup>+</sup>CD1d<sup>hi</sup> or CD138<sup>+</sup>, n = 3-4/group.

proportion of CD5<sup>+</sup>CD1d<sup>hi</sup> cells in the Cnp-Mek1DD mice correlated with a significant increase in the expression of IL-10, which is the cytokine that B10 cells must produce in order to elicit an immunosuppressive effect in EAE. Therefore, we ran qRT-PCR for IL-10 using RNA isolated from LPS-stimulated control and Cnp-Mek1DD

B-cells. We observed a 3-fold significant increase in IL-10 transcription from Cnp-Mek1DD LPS-stimulated B-cells compared to controls (Figure 7F; normalized to control, Cnp-Mek1DD = 3.05; p = 0.009). While published data indicate that LPS stimulation results in the expansion of IL-10 producing B10 cells, IL-10 production by these cells is further increased with the addition of phorbol 12-myristate 13-acetate (PMA) and ionomycin in the last 5 hrs. of culture (Yanaba et al., 2008). Based on this, we also isolated RNA from LPS and PMA+ionomycin (PI)-stimulated control and Cnp-Mek1DD B-cells. qRT-PCR analysis revealed that while control B-cells upregulated IL-10 transcription, this increase in expression was significantly higher in Cnp-Mek1DD B-cells (Figure 7F; normalized to LPS-stimulated control, Control = 4.12, Cnp-Mek1DD = 7.23; p = 0.05). We then used an ELISA assay to determine whether B-cells from Cnp-Mek1DD mice secreted more IL-10 into the culture media over 48 hours in response to stimulation. While LPS stimulation alone did not result in increased IL-10 secretion (Figure 7G; Control = 533.4 pg/mL, Cnp-Mek1DD = 595 pg/mL; p = 0.73), media from LPS+PI-stimulated Cnp-Mek1DD B-cells exhibited a significant increase in IL-10 levels compared to control media (Figure 7G; Control = 838.3 pg/mL, Cnp-Mek1DD = 1231 pg/mL; p = 0.02). Taken together, these data support the conclusion that the increased response to LPS stimulation by Cnp-Mek1DD B-cells results in enhanced expansion of IL-10 producing B-cell subsets, such as B10 cells, and upregulation of anti-inflammatory cytokine IL-10 transcription and secretion after LPS+PI stimulation.

## Discussion

The ERK1/2 signaling pathway was previously implicated in regulating remyelination efficiency and thickness, with mice lacking ERK2 in the OL lineage displaying delayed remyelination and mice expressing MEK1DD in the OL lineage exhibiting accelerated remyelination with thicker myelin sheaths after LPC demyelination (Fyffe-Maricich et al., 2013; Michel et al., 2015). With the impressive results from these LPC studies in Cnp-Mek1DD mice, we wanted to examine how MEK1DD expression in the OL lineage might affect immune-mediated de- and remyelination. Strikingly, we observed a significant improvement in EAE disease course and white matter lesion load in Cnp-Mek1DD mice compared to controls. However, we were surprised when experiments using Plp-Mek1DD mice indicated that ERK1/2 activation in existing OLs during demyelination did not also protect against EAE induction. Instead, our data suggest an important role for ERK1/2 signaling in immune cells, particularly CD19<sup>+</sup> splenic B-cells, which may modulate EAE severity.

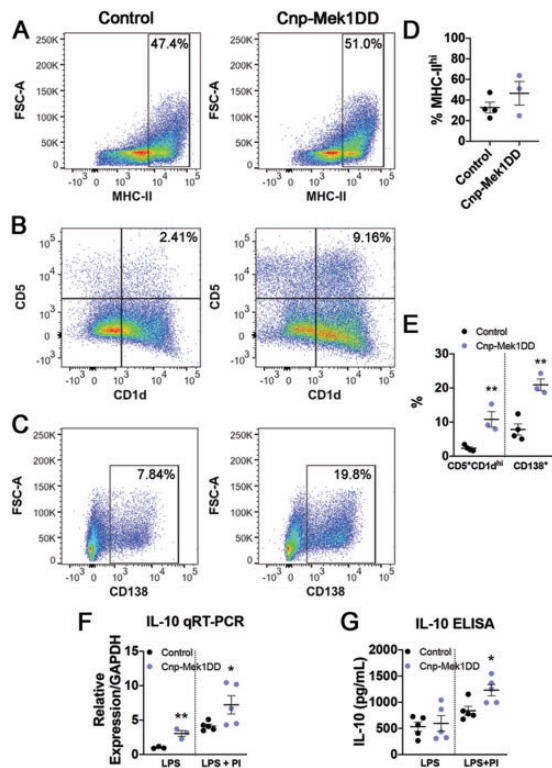


**Figure 7.** MEK1DD Expression Results in Increased B-Cell Activation After *In Vitro* LPS Stimulation. **A:** Representative flow cytometry dot plots from control and GFP<sup>+</sup> LPS-stimulated B-cells showing MHC-II<sup>hi</sup> B-cells, *n* = 3-4/group. **B:** Representative flow cytometry dot plots from control and GFP<sup>+</sup> LPS-stimulated B-cells showing CD5<sup>+</sup>CD1d<sup>hi</sup> B-cells, *n* = 3-4/group. **C:** Representative flow cytometry dot plots from control and GFP<sup>+</sup> LPS stimulated B-cells showing CD138<sup>+</sup> plasmablasts, *n* = 3-4/group. **D:** Graph of the % of CD19<sup>+</sup> cells that are high-expressing MHC-II in control and Cnp-Mek1DD GFP<sup>+</sup> LPS-stimulated B-cells, *n* = 3-4/group. **E:** Graph of the % of CD19<sup>+</sup> B-cells that are CD5<sup>+</sup>CD1d<sup>hi</sup> or CD138<sup>+</sup> in control and Cnp-Mek1DD GFP<sup>+</sup> LPS stimulated B-cells, *n* = 3-4/group. **F:** Relative mRNA expression of IL-10 in LPS-stimulated or LPS+PI-stimulated control and Cnp-Mek1DD GFP<sup>+</sup> B-cells, *n* = 3-5/group. \**p* ≤ 0.05, \*\**p* ≤ 0.01.

Our data showing no difference in clinical EAE score severity in Plp-Mek1DD mice given tamoxifen prior to EAE induction compared to controls suggests that the functional protection exhibited by Cnp-Mek1DD mice is not due to hypermyelination. It is important to note that our data, in line with previous studies, indicates the extent of hypermyelination is greater in Cnp-Mek1DD mice compared to Plp-Mek1DD mice (Fyffe-Maricich et al., 2013; Ishii et al., 2013; 2016; Jeffries et al., 2016). Although we initially hypothesized that hypermyelination would be protective against EAE, existing data suggest that extreme hypermyelination similar to that seen in Cnp-Mek1DD mice can exacerbate EAE severity (Jaini et al., 2013). Therefore, while we cannot rule out the possibility that hypermyelination in Cnp-Mek1DD mice

could synergistically provide protection against EAE, it is likely that immune modulation is the chief factor in the observed suppression of EAE clinical scores.

Pdgfr $\alpha$ -Mek1DD mice given tamoxifen to induce MEK1DD expression in OPCs during EAE had similar disease course to controls, suggesting that enhanced ERK signaling in adult OPCs, and the population of remyelinating OLs that they give rise to, is not sufficient to lead to functional improvements in the context of immune-mediated demyelination. Additionally, Plp-Mek1DD mice did not exhibit functional improvement despite existing evidence that pre-existing mature OLs expressing MEK1DD can contribute to remyelination after LPC demyelination (Jeffries et al., 2016). Conversely, Cnp-Mek1DD mice showed significantly better functional improvement in EAE score compared to controls, along with the initial reduction in EAE severity. It is possible that the inflammatory environment of EAE and ongoing demyelination may functionally override any improvement on remyelination thickness, such that even if Pdgfr $\alpha$ -Mek1DD or Plp-Mek1DD mice do exhibit thicker remyelination similar to that observed in Cnp-Mek1DD mice after LPC injection (Fyffe-Maricich et al., 2013), it is not sufficient to alter clinical EAE score. This is possible since it has been shown that inflammation and axonal pathology contribute heavily to functional impairment in EAE (Wujek et al., 2002; Lassmann & Bradl, 2017). We further cannot eliminate the possibility that it is a combination of improved remyelination and altered immunological response that results in the improved EAE phenotype of Cnp-Mek1DD mice. Experiments dissecting the potential contributions of immune cell modulation and improved remyelination to either the observed suppression of EAE disease progression or the improvement of EAE functional score will be of importance in future studies.

*Cnp-Cre* mice until now have been used as an OL lineage and Schwann cell-specific Cre mouse line. However, there have been previous reports of *Cnp* gene expression in cells outside the CNS, which the original study using *Cnp-Cre* mice mentioned in brief (Lappe-Siefke et al., 2003). Mouse ENCODE Consortium transcriptome data reveals high levels of *Cnp* transcription in adult spleen and thymus along with brain tissues (F. Yue et al., 2014). Additionally, a study using Northern blotting to examine *Cnp1* transcription in mouse tissues showed that while expression is highest in the brain, *Cnp1* expression is also evident in spleen, heart, liver, and lung (Miyoshi et al., 2001). Another study demonstrated that CNPase activity appears to be highest outside of the CNS in the spleen and thymus (Weissbarth et al., 1981). More specifically, a study examining CNPase enzymatic activity revealed that while myelin indeed displays the highest level of CNPase activity, both human and rat lymphocytes exhibit measurable

CNPase activity (Sheedlo et al., 1984). Finally, human lymphocytes showed increased CNPase activity *in vitro* when stimulated with a mitogenic lectin from *Robinia pseudoacacia*, although curiously, the researchers did not observe a significant increase in CNPase activity when stimulating fractionated T-cells or B-cells alone (Sabeur et al., 1986). These studies strongly support our conclusion that the *Cnp* promoter is active and drives CRE expression in splenic immune cells. While previously undescribed in studies using the *Cnp-Cre* mouse, it will be of critical importance to consider immune cell function when using *Cnp-Cre* mice in future research.

Despite the knowledge that CNPase is expressed and active in splenic tissues and immune cells, EAE studies using mice with gene expression or deletion driven by the *Cnp* promoter have variably addressed this. When pancreatic ER kinase (PERK) is deleted using *Cnp-Cre*, this results in detectable loxP recombination in tail, heart, and lung tissue in addition to the brain, but not in spleen or thymus, in contrast to our data using GFP expression (Hussien et al., 2014). While these mice display worsened EAE, no change in T-cell infiltration or macrophage/microglial activation was observed. Similarly, PCR analysis of activating transcription factor 4 (ATF4) deletion using *Cnp-Cre* in a second publication did not reveal loxP recombination in any tissue outside of the CNS, and these mice displayed comparable EAE disease to controls (Y. Yue et al., 2019). A third publication demonstrated striking attenuation of EAE severity in adult *Cnp-Cre;Chrm1<sup>fl/fl</sup>* mice without effect on developmental myelination, but potential effects on immune function were not addressed (Mei et al., 2016). Another study used *Cnp-Cre* to delete tumor necrosis factor receptor 2 (TNFR2), resulting in exacerbated EAE disease course (Madsen et al., 2016). Interestingly, in this report the researchers observed increased T-cell infiltration during peak disease, but did not investigate whether recombination occurred in immune cell populations. In a publication using *Cnp-Cre* to express ovalbumin (OVA) neoepitopes, adoptive transfer of OVA-specific T-cells worsened EAE severity; these mice displayed increased T-cell infiltration and myeloid cell numbers but no analysis of potential recombination in host immune cell populations was performed (Rayasam et al., 2018). One study used the *Cnp* expression cassette, rather than *Cnp-Cre*, to express dominant negative interferon regulatory factor 1 (IRF-1), resulting in strongly attenuated EAE disease course (Ren et al., 2011). Importantly, this study validated CNS-specific expression of the dominant negative IRF-1 downstream of the *Cnp* expression cassette, and no changes in peripheral immune cell populations or function were observed. The variable data on immune cell recombination when using the *Cnp* promoter in EAE studies further underscore the

importance of considering potential changes to immune function in these models.

Our results indicate that *Cnp-Mek1DD* spleens exhibit approximately 70% CD19<sup>+</sup> B-cell recombination, 30% CD11b<sup>+</sup> monocyte recombination, 25% CD4<sup>+</sup> T-cell recombination, and 30% CD8<sup>+</sup> T-cell recombination. However, Plp-DR mice did not demonstrate splenic recombination, suggesting that Plp-Mek1DD mice, unlike *Cnp-Mek1DD* mice, do not have MEK1DD-expressing splenic immune cells during EAE that may be contributing to suppression of EAE disease initiation. *Cnp-Mek1DD* mice revealed reduced EAE clinical severity versus controls while Plp-Mek1DD EAE scores were comparable to controls. Therefore, the decrease in severity of EAE clinical scores observed in *Cnp-Mek1DD* mice is likely being driven primarily by altered immune cell function and not enhanced ERK1/2 signaling in the OL-lineage. Previous literature has revealed ERK1/2 signaling promotes the activation of CD4<sup>+</sup> T-cells thought to be primarily responsible for EAE induction, while also driving activation of cytotoxic CD8<sup>+</sup> T-cells and suppressing and destabilizing CD4<sup>+</sup>FoxP3<sup>+</sup> regulatory T-cells (Dumont et al., 1998; D'Souza et al., 2008; Luo et al., 2008; Chang et al., 2012; Liu et al., 2013; Guo et al., 2014). In particular, ERK1/2 signaling has been shown in several studies to activate EAE-inducing Th1 and Th17 cells (Chang et al., 2012; Liu et al., 2013). In addition, ERK1/2 signaling has been widely studied in macrophage development and activation, with evidence for ERK1/2 activation promoting proinflammatory polarization (Rao, 2001; Traves et al., 2012). Because the expression of MEK1DD results in sustained ERK1/2 activation, it seems unlikely that recombined monocyte or T-cell populations in *Cnp-Mek1DD* mice are the cause of reduced EAE severity. However, it is important to note that we cannot eliminate the possibility that effects on these cell populations contribute to the observed effect on EAE disease course. Therefore, future studies will need to examine the role of ERK1/2 signaling in *Cnp-Mek1DD* T-cells and macrophages during EAE.

With the recent clinical success of B-cell targeted drugs like Ocrevus and Rituximab, there has been increasing interest in the roles of various B-cell populations in MS. Studies using the EAE model of demyelination have revealed mixed results in regard to B-cell necessity and function. While some reports have suggested that B-cells are unnecessary for EAE induction and progression, others have shown important modulatory roles for B-cells in EAE disease (Mann et al., 2012; Pierson et al., 2014; Ray & Basu, 2014; Parker Harp et al., 2015; Hausser-Kinzel & Weber, 2019). In addition to this, previous work has highlighted the importance of ERK1/2 signaling in B-cell development and activation, with B-cell Receptor (BCR) ligation resulting in ERK1/2 activation (Richards et al., 2001; Jacob et al., 2002; Rui et al.,

2006; Gold, 2008; Teodorovic et al., 2014; Adem et al., 2015). When stimulated *in vitro*, B-cells expressing MEK1DD exhibited increased numbers of CD5<sup>+</sup>CD1d<sup>hi</sup> B-cells as well as CD138<sup>+</sup> plasmablasts, along with significantly upregulated IL-10 transcription and secretion. Previous research has found that both regulatory B10 cells, associated with the CD5<sup>+</sup>CD1d<sup>hi</sup> subset, as well as CD138<sup>+</sup> plasmablasts are able to secrete IL-10 (Matsushita et al., 2008, 2010; Matsumoto et al., 2014; Shen et al., 2014; Rojas et al., 2019). Multiple studies have shown the importance of IL-10 in modulating EAE severity (Bettelli et al., 1998; Xiao et al., 1998; Cua et al., 1999). In particular, increased IL-10 expression by regulatory B10 cells has been shown to inhibit the development of EAE disease in a pattern similar to that observed in Cnp-Mek1DD mice, despite low B-cell infiltration into the CNS (Matsushita et al., 2010; Mann et al., 2012). Excitingly, very recent publications demonstrate that the adoptive transfer of IL-10 producing regulatory B10 cells results in immunosuppression and concurrently promotes oligodendrogenesis and remyelination in the EAE model (Pennati et al., 2016; 2020). ERK1/2 signaling has been implicated in IL-10 expression in multiple cell types (Saraiva & O'Garra, 2010; Iyer & Cheng, 2012; Kubo & Motomura, 2012; Sanin et al., 2015; Garaud et al., 2018; Zhang & Kuchroo, 2019). Of particular interest are data revealing that in both human and mouse B-cells, TLR-mediated ERK1/2 activation is critical to induce IL-10 production, suggesting that the expression of MEK1DD may directly upregulate IL-10 transcription in splenic B-cells (Liu et al., 2014; Sutavani et al., 2018). Taken together, these data suggest that ERK1/2 signaling promotes splenic B-cell activation and the expansion of CD5<sup>+</sup>CD1d<sup>hi</sup> and CD138<sup>+</sup> B-cell subsets, and may drive IL-10 expression in one or both of these populations.

This study presents novel data indicating that *Cnp-Cre* drives recombination in splenic immune cell populations, in particular CD19<sup>+</sup> B-cells. Additionally, we determined that sustained ERK1/2 signaling in splenic B-cells results in enhanced activation of CD5<sup>+</sup>CD1d<sup>hi</sup> and CD138<sup>+</sup> subsets of B-cells and increased IL-10 expression, which may contribute to the inhibition of MOG<sub>35-55</sub> EAE disease progression. In conclusion, our data support the concept that downstream effectors of the ERK1/2 signaling pathway modulating B-cell function may be potential therapeutic targets in immune-mediated demyelinating diseases such as MS.

## Summary Statement

ERK1/2 activation solely in oligodendrocyte-lineage cells does not provide a functional benefit in the context of EAE-mediated demyelination. Sustained ERK1/2 activation in both OL-lineage as well as B-cells, however,

results in increased IL-10 expression and the attenuation of immune-mediated demyelination.

## Acknowledgments

The authors would like to thank Dr. Wendy Macklin, Luipa Khandker, and Angelina Evangelou for helpful discussions and comments on this manuscript. We would like to thank Mara Sullivan and the Center for Biologic Imaging at the University of Pittsburgh for the thick toluidine blue sections. We also thank Tammy Mui-Galenkamp and the NJMS Flow Cytometry and Immunology Core Laboratory for the flow sorting to isolate CD19<sup>+</sup> B-cells, as well as Dr. Sukhwinder Singh for his valuable expertise with flow cytometry.

## Author Contributions

M. A. J., S. L. F.-M., and T. L. W. designed research; M. A. J., A. E. O., and K. U. performed research; M. A. J., A. E. O., and K. U. analyzed data; M. A. J., A. E. O., S. L. F.-M., and T. L. W. wrote the paper.




## Declaration of Conflicting Interests

The author(s) declared no potential conflicts of interest with respect to the research, authorship, and/or publication of this article.

## Funding

The author(s) disclosed receipt of the following financial support for the research, authorship, and/or publication of this article: This work was supported by an NMSS-Career Transition Fellowship to S. L. F.-M., NIH R01 NS091084 to S. L. F.-M., NIH R01 NS082203 to T. L. W., NMSS RG170728557 to T. L. W., and NIH F31 NS108521 to M. A. J.

## ORCID iDs

Marisa A. Jeffries  <https://orcid.org/0000-0002-2486-0457>  
 Alison E. Obr  <https://orcid.org/0000-0003-0949-3131>  
 Teresa L. Wood  <https://orcid.org/0000-0002-4480-660X>

## Supplemental Material

Supplementary material for this article is available online.

## References

- Adem, J., Hamalainen, A., Ropponen, A., Eeva, J., Eray, M., Nuutinen, U., & Pelkonen, J. (2015). ERK1/2 has an essential role in B cell receptor- and CD40-induced signaling in an *in vitro* model of germinal center B cell selection. *Molecular Immunology*, 67(2 Pt B), 240–247.
- Bettelli, E., Das, M. P., Howard, E. D., Weiner, H. L., Sobel, R. A., & Kuchroo, V. K. (1998). IL-10 is critical in the regulation of autoimmune encephalomyelitis as demonstrated by studies of IL-10- and IL-4-deficient and transgenic mice. *Journal of Immunology (Baltimore, MD: 1950)*, 161(7), 3299–3306.
- Chang, C. F., D'Souza, W. N., Ch'en, I. L., Pages, G., Pouyssegur, J., & Hedrick, S. M. (2012). Polar opposites: Erk direction of CD4 T cell subsets. *Journal of Immunology (Baltimore, MD: 1950)*, 189(2), 721–731.

- Chen, D., Ireland, S. J., Davis, L. S., Kong, X., Stowe, A. M., Wang, Y., White, W. I., Herbst, R., & Monson, N. L. (2016). Autoreactive CD19+CD20- Plasma cells contribute to disease severity of experimental autoimmune encephalomyelitis. *Journal of Immunology (Baltimore, MD: 1950)*, *196*(4), 1541–1549.
- Cua, D. J., Groux, H., Hinton, D. R., Stohlman, S. A., & Coffman, R. L. (1999). Transgenic interleukin 10 prevents induction of experimental autoimmune encephalomyelitis. *The Journal of Experimental Medicine*, *189*(6), 1005–1010.
- Davidoff, M. S., Middendorff, R., Kofuncu, E., Muller, D., Jezek, D., & Holstein, A. F. (2002). Leydig cells of the human testis possess astrocyte and oligodendrocyte marker molecules. *Acta Histochemica*, *104*(1), 39–49.
- Doerflinger, N. H., Macklin, W. B., & Popko, B. (2003). Inducible site-specific recombination in myelinating cells. *Genesis (New York, N.Y.: 2000)*, *35*(1), 63–72.
- D'Souza, W. N., Chang, C. F., Fischer, A. M., Li, M., & Hedrick, S. M. (2008). The Erk2 MAPK regulates CD8 T cell proliferation and survival. *Journal of Immunology (Baltimore, MD: 1950)*, *181*(11), 7617–7629.
- Dumont, F. J., Staruch, M. J., Fischer, P., DaSilva, C., & Camacho, R. (1998). Inhibition of T cell activation by pharmacologic disruption of the MEK1/ERK MAP kinase or calcineurin signaling pathways results in differential modulation of cytokine production. *Journal of Immunology (Baltimore, MD: 1950)*, *160*(6), 2579–2589.
- Fillatreau, S. (2019). Regulatory functions of B cells and regulatory plasma cells. *Biomedical Journal*, *42*(4), 233–242.
- Funfschilling, U., Supplie, L. M., Mahad, D., Boretius, S., Saab, A. S., Edgar, J., Brinkmann, B. G., Kassmann, C. M., Tzvetanova, I. D., Mobius, W., Diaz, F., Meijer, D., Suter, U., Hamprecht, B., Sereda, M. W., Moraes, C. T., Frahm, J., Goebbels, S., & Nave, K. A. (2012). Glycolytic oligodendrocytes maintain myelin and long-term axonal integrity. *Nature*, *485*(7399), 517–521.
- Fyffe-Maricich, S. L., Schott, A., Karl, M., Krasno, J., & Miller, R. H. (2013). Signaling through ERK1/2 controls myelin thickness during myelin repair in the adult central nervous system. *The Journal of Neuroscience: The Official Journal of the Society for Neuroscience*, *33*(47), 18402–18408.
- Garaud, S., Taher, T. E., Debant, M., Burgos, M., Melayah, S., Berthou, C., Parikh, K., Pers, J. O., Luque-Paz, D., Chiocchia, G., Peppelenbosch, M., Isenberg, D. A., Youinou, P., Mignen, O., Renaudineau, Y., & Mageed, R. A. (2018). CD5 expression promotes IL-10 production through activation of the MAPK/erk pathway and upregulation of TRPC1 channels in B lymphocytes. *Cellular & Molecular Immunology*, *15*(2), 158–170.
- Gold, M. R. (2008). B cell development: Important work for ERK. *Immunity*, *28*(4), 488–490.
- Guo, J., Zhang, J., Zhang, X., Zhang, Z., Wei, X., & Zhou, X. (2014). Constitutive activation of MEK1 promotes treg cell instability in vivo. *The Journal of Biological Chemistry*, *289*(51), 35139–35148.
- Hausser-Kinzel, S., & Weber, M. S. (2019). The role of B cells and antibodies in multiple sclerosis, neuromyelitis optica, and related disorders. *Frontiers in Immunology*, *10*, 201.
- Hussien, Y., Cavener, D. R., & Popko, B. (2014). Genetic inactivation of PERK signaling in mouse oligodendrocytes: Normal developmental myelination with increased susceptibility to inflammatory demyelination. *Glia*, *62*(5), 680–691.
- Ishii, A., Furusho, M., & Bansal, R. (2013). Sustained activation of ERK1/2 MAPK in oligodendrocytes and schwann cells enhances myelin growth and stimulates oligodendrocyte progenitor expansion. *The Journal of Neuroscience: The Official Journal of the Society for Neuroscience*, *33*(1), 175–186.
- Ishii, A., Furusho, M., Dupree, J. L., & Bansal, R. (2016). Strength of ERK1/2 MAPK activation determines its effect on myelin and axonal integrity in the adult CNS. *The Journal of Neuroscience: The Official Journal of the Society for Neuroscience*, *36*(24), 6471–6487.
- Ishii, A., Fyffe-Maricich, S. L., Furusho, M., Miller, R. H., & Bansal, R. (2012). ERK1/ERK2 MAPK signaling is required to increase myelin thickness independent of oligodendrocyte differentiation and initiation of myelination. *The Journal of Neuroscience: The Official Journal of the Society for Neuroscience*, *32*(26), 8855–8864.
- Iyer, S. S., & Cheng, G. (2012). Role of interleukin 10 transcriptional regulation in inflammation and autoimmune disease. *Critical Reviews in Immunology*, *32*(1), 23–63.
- Jacob, A., Cooney, D., Pradhan, M., & Coggeshall, K. M. (2002). Convergence of signaling pathways on the activation of ERK in B cells. *The Journal of Biological Chemistry*, *277*(26), 23420–23426.
- Jager, A., Dardalhon, V., Sobel, R. A., Bettelli, E., & Kuchroo, V. K. (2009). Th1, Th17, and Th9 effector cells induce experimental autoimmune encephalomyelitis with different pathological phenotypes. *Journal of Immunology (Baltimore, MD: 1950)*, *183*(11), 7169–7177.
- Jaini, R., Popescu, D. C., Flask, C. A., Macklin, W. B., & Tuohy, V. K. (2013). Myelin antigen load influences antigen presentation and severity of central nervous system autoimmunity. *Journal of Neuroimmunology*, *259*(1-2), 37–46.
- Jeffries, M. A., Urbanek, K., Torres, L., Wendell, S. G., Rubio, M. E., & Fyffe-Maricich, S. L. (2016). ERK1/2 activation in preexisting oligodendrocytes of adult mice drives new myelin synthesis and enhanced CNS function. *The Journal of Neuroscience: The Official Journal of the Society for Neuroscience*, *36*(35), 9186–9200.
- Joseph, S., Vingill, S., Jahn, O., Fledrich, R., Werner, H. B., Katona, I., Mobius, W., Mitkovski, M., Huang, Y., Weis, J., Sereda, M. W., Schulz, J. B., Nave, K. A., & Stegmuller, J. (2019). Myelinating glia-specific deletion of Fbxo7 in mice triggers axonal degeneration in the central nervous system together with peripheral neuropathy. *The Journal of Neuroscience: The Official Journal of the Society for Neuroscience*, *39*(28), 5606–5626.
- Kang, S. H., Fukaya, M., Yang, J. K., Rothstein, J. D., & Bergles, D. E. (2010). NG2+ CNS glial progenitors remain committed to the oligodendrocyte lineage in postnatal life and following neurodegeneration. *Neuron*, *68*(4), 668–681.
- Kubo, M., & Motomura, Y. (2012). Transcriptional regulation of the anti-inflammatory cytokine IL-10 in acquired immune cells. *Frontiers in Immunology*, *3*, 275.

- Lappe-Siefke, C., Goebbels, S., Gravel, M., Nicksch, E., Lee, J., Braun, P. E., Griffiths, I. R., & Nave, K. A. (2003). Disruption of Cnpl uncouples oligodendroglial functions in axonal support and myelination. *Nature Genetics*, *33*(3), 366–374.
- Lassmann, H., & Bradl, M. (2017). Multiple sclerosis: Experimental models and reality. *Acta Neuropathologica*, *133*(2), 223–244.
- Liu, B. S., Cao, Y., Huizinga, T. W., Hafler, D. A., & Toes, R. E. (2014). TLR-mediated STAT3 and ERK activation controls IL-10 secretion by human B cells. *European Journal of Immunology*, *44*(7), 2121–2129.
- Liu, H., Yao, S., Dann, S. M., Qin, H., Elson, C. O., & Cong, Y. (2013). ERK differentially regulates Th17- and treg-cell development and contributes to the pathogenesis of colitis. *European Journal of Immunology*, *43*(7), 1716–1726.
- Luo, X., Zhang, Q., Liu, V., Xia, Z., Pothoven, K. L., & Lee, C. (2008). Cutting edge: TGF-beta-induced expression of Foxp3 in T cells is mediated through inactivation of ERK. *Journal of Immunology (Baltimore, MD: 1950)*, *180*(5), 2757–2761.
- Lyons, J. A., San, M., Happ, M. P., & Cross, A. H. (1999). B cells are critical to induction of experimental allergic encephalomyelitis by protein but not by a short encephalitogenic peptide. *Eur J Immunol*, *29*(11), 3432–3439. [https://doi.org/10.1002/\(SICI\)1521-4141\(199911\)29:11<3432::AID-IMMU3432>3.0.CO;2-2](https://doi.org/10.1002/(SICI)1521-4141(199911)29:11<3432::AID-IMMU3432>3.0.CO;2-2)
- Madsen, P. M., Motti, D., Karmally, S., Szymkowski, D. E., Lambertsen, K. L., Bethea, J. R., & Brambilla, R. (2016). Oligodendroglial TNFR2 mediates membrane TNF-Dependent repair in experimental autoimmune encephalomyelitis by promoting oligodendrocyte differentiation and remyelination. *The Journal of Neuroscience: The Official Journal of the Society for Neuroscience*, *36*(18), 5128–5143.
- Mann, M. K., Ray, A., Basu, S., Karp, C. L., & Dittel, B. N. (2012). Pathogenic and regulatory roles for B cells in experimental autoimmune encephalomyelitis. *Autoimmunity*, *45*(5), 388–399.
- Matsumoto, M., Baba, A., Yokota, T., Nishikawa, H., Ohkawa, Y., Kayama, H., Kallies, A., Nutt, S. L., Sakaguchi, S., Takeda, K., Kurosaki, T., & Baba, Y. (2014). Interleukin-10-producing plasmablasts exert regulatory function in autoimmune inflammation. *Immunity*, *41*(6), 1040–1051.
- Matsushita, T., Horikawa, M., Iwata, Y., & Tedder, T. F. (2010). Regulatory B cells (B10 cells) and regulatory T cells have independent roles in controlling experimental autoimmune encephalomyelitis initiation and late-phase immunopathogenesis. *Journal of Immunology (Baltimore, MD: 1950)*, *185*(4), 2240–2252.
- Matsushita, T., Yanaba, K., Bouaziz, J. D., Fujimoto, M., & Tedder, T. F. (2008). Regulatory B cells inhibit EAE initiation in mice while other B cells promote disease progression. *The Journal of Clinical Investigation*, *118*(10), 3420–3430.
- McFerran, B., & Burgoyne, R. (1997). 2',3'-Cyclic nucleotide 3'-phosphodiesterase is associated with mitochondria in diverse adrenal cell types. *Journal of Cell Science*, *110*(Pt 23), 2979–2985.
- Mei, F., Lehmann-Horn, K., Shen, Y.-A. A., Rankin, K. A., Stebbins, K. J., Lorrain, D. S., Pekarek, K., A Sagan, S., Xiao, L., Teuscher, C., von Büdingen, H.-C., Wess, J., Lawrence, J. J., Green, A. J., Fancy, S. P., Zamvil, S. S., & Chan, J. R. (2016). Accelerated remyelination during inflammatory demyelination prevents axonal loss and improves functional recovery. *Elife*, *5*. <https://doi.org/10.7554/eLife.18246>
- Mendel, I., Kerlero de Rosbo, N., & Ben-Nun, A. (1995). A myelin oligodendrocyte glycoprotein peptide induces typical chronic experimental autoimmune encephalomyelitis in H-2b mice: Fine specificity and T cell receptor V beta expression of encephalitogenic T cells. *European Journal of Immunology*, *25*(7), 1951–1959.
- Meyer, N., Richter, N., Fan, Z., Siemonsmeier, G., Pivneva, T., Jordan, P., Steinhauser, C., Semtner, M., Nolte, C., & Kettenmann, H. (2018). Oligodendrocytes in the mouse corpus callosum maintain axonal function by delivery of glucose. *Cell Reports*, *22*(9), 2383–2394.
- Michel, K., Zhao, T., Karl, M., Lewis, K., & Fyffe-Maricich, S. L. (2015). Translational control of myelin basic protein expression by ERK2 MAP kinase regulates timely remyelination in the adult brain. *The Journal of Neuroscience: The Official Journal of the Society for Neuroscience*, *35*(20), 7850–7865.
- Miyoshi, K., Cui, Y., Riedlinger, G., Robinson, P., Lehoczyk, J., Zon, L., Oka, T., Dewar, K., & Hennighausen, L. (2001). Structure of the mouse stat 3/5 locus: Evolution from drosophila to zebrafish to mouse. *Genomics*, *71*(2), 150–155.
- Muzumdar, M. D., Tasic, B., Miyamichi, K., Li, L., & Luo, L. (2007). A global double-fluorescent cre reporter mouse. *Genesis (New York, N.Y.: 2000)*, *45*(9), 593–605.
- Nishizawa, Y., Kurihara, T., Masuda, T., & Takahashi, Y. (1985). Immunohistochemical localization of 2',3'-cyclic nucleotide 3'-phosphodiesterase in adult bovine cerebrum and cerebellum. *Neurochemical Research*, *10*(8), 1107–1118.
- Okuda, Y., Sakoda, S., Fujimura, H., Saeki, Y., Kishimoto, T., & Yanagihara, T. (1999). IL-6 plays a crucial role in the induction phase of myelin oligodendrocyte glycoprotein 35-55 induced experimental autoimmune encephalomyelitis. *Journal of Neuroimmunology*, *101*(2), 188–196. [https://doi.org/10.1016/S0165-5728\(99\)00139-3](https://doi.org/10.1016/S0165-5728(99)00139-3)
- Pachynski, R. K., Scholz, A., Monnier, J., Butcher, E. C., & Zabel, B. A. (2015). Evaluation of tumor-infiltrating leukocyte subsets in a subcutaneous tumor model. *Journal of Visualized Experiments*, *98*, e52657.
- Parker Harp, C. R., Archambault, A. S., Sim, J., Ferris, S. T., Mikesell, R. J., Koni, P. A., Shimoda, M., Lington, C., Russell, J. H., & Wu, G. F. (2015). B cell antigen presentation is sufficient to drive neuroinflammation in an animal model of multiple sclerosis. *Journal of Immunology (Baltimore, MD: 1950)*, *194*(11), 5077–5084.
- Pennati, A., Ng, S., Wu, Y., Murphy, J. R., Deng, J., Rangaraju, S., Asress, S., Blanchfield, J. L., Evavold, B., & Galipeau, J. (2016). Regulatory B cells induce formation of IL-10-Expressing T cells in mice with autoimmune neuroinflammation. *The Journal of Neuroscience: The Official Journal of the Society for Neuroscience*, *36*(50), 12598–12610.



- Pennati, A., Nylen, E. A., Duncan, I. D., & Galipeau, J. (2020). Regulatory B cells normalize CNS myeloid cell content in a mouse model of multiple sclerosis and promote oligodendrocyte maturation and remyelination. *The Journal of Neuroscience: The Official Journal of the Society for Neuroscience*, *40*(26), 5105–5115.
- Pierson, E. R., Stromnes, I. M., & Goverman, J. M. (2014). B cells promote induction of experimental autoimmune encephalomyelitis by facilitating reactivation of T cells in the central nervous system. *Journal of Immunology (Baltimore, MD: 1950)*, *192*(3), 929–939.
- Pollok, K., Mothes, R., Ulbricht, C., Liebheit, A., Gerken, J. D., Uhlmann, S., Paul, F., Niesner, R., Radbruch, H., & Hauser, A. E. (2017). The chronically inflamed central nervous system provides niches for long-lived plasma cells. *Acta Neuropathologica Communications*, *5*(1), 88.
- Rangachari, M., & Kuchroo, V. K. (2013). Using EAE to better understand principles of immune function and autoimmune pathology. *Journal of Autoimmunity*, *45*, 31–39.
- Rao, K. M. (2001). MAP kinase activation in macrophages. *Journal of Leukocyte Biology*, *69*(1), 3–10.
- Ray, A., & Basu, S. (2014). Regulatory B cells in experimental autoimmune encephalomyelitis (EAE). *Methods in Molecular Biology (Clifton, N.J.)*, *1190*, 243–255.
- Rayasam, A., Kijak, J. A., Dallmann, M., Hsu, M., Zindl, N., Lindstedt, A., Steinmetz, L., Harding, J. S., Harris, M. G., Karman, J., Sandor, M., & Fabry, Z. (2018). Regional distribution of CNS antigens differentially determines T-Cell mediated neuroinflammation in a CX3CR1-Dependent manner. *The Journal of Neuroscience: The Official Journal of the Society for Neuroscience*, *38*(32), 7058–7071.
- Ren, Z., Wang, Y., Tao, D., Liebenson, D., Liggett, T., Goswami, R., Clarke, R., Stefoski, D., & Balabanov, R. (2011). Overexpression of the dominant-negative form of interferon regulatory factor 1 in oligodendrocytes protects against experimental autoimmune encephalomyelitis. *The Journal of Neuroscience: The Official Journal of the Society for Neuroscience*, *31*(23), 8329–8341.
- Richards, J. D., Dave, S. H., Chou, C. H., Mamchak, A. A., & DeFranco, A. L. (2001). Inhibition of the MEK/ERK signaling pathway blocks a subset of B cell responses to antigen. *Journal of Immunology (Baltimore, MD: 1950)*, *166*(6), 3855–3864.
- Rojas, O. L., Pröbstel, A.-K., Porfilio, E. A., Wang, A. A., Charabati, M., Sun, T., Lee, D. S. W., Galicia, G., Ramaglia, V., Ward, L. A., Leung, L. Y. T., Najafi, G., Khaleghi, K., Garcillán, B., Li, A., Besla, R., Naouar, I., Cao, E. Y., Chiaranunt, P., . . . Gommerman, J. L. (2019). Recirculating intestinal IgA-Producing cells regulate neuroinflammation via IL-10. *Cell*, *177*(2), 492–493.
- Rui, L., Healy, J. I., Blasioli, J., & Goodnow, C. C. (2006). ERK signaling is a molecular switch integrating opposing inputs from B cell receptor and T cell cytokines to control TLR4-driven plasma cell differentiation. *Journal of Immunology (Baltimore, MD: 1950)*, *177*(8), 5337–5346.
- Sabeur, G., Wantyghem, J., & Schuller, E. (1986). Stimulation of 2',3'-cyclic nucleotide 3'-phosphodiesterase in human lymphocytes by robinia pseudoacacia lectin. *Biochimie*, *68*(4), 581–585.
- Samoilova, E. B., Horton, J. L., Hilliard, B., Liu, T. S., & Chen, Y. (1998). IL-6-deficient mice are resistant to experimental autoimmune encephalomyelitis: Roles of IL-6 in the activation and differentiation of autoreactive T cells. *Journal of Immunology (Baltimore, MD: 1950)*, *161*(12), 6480–6486.
- Sanin, D. E., Prendergast, C. T., & Mountford, A. P. (2015). IL-10 production in macrophages is regulated by a TLR-Driven CREB-Mediated mechanism that is linked to genes involved in cell metabolism. *Journal of Immunology (Baltimore, MD: 1950)*, *195*(3), 1218–1232.
- Saraiva, M., & O'Garra, A. (2010). The regulation of IL-10 production by immune cells. *Nature Reviews. Immunology*, *10*(3), 170–181.
- Serada, S., Fujimoto, M., Mihara, M., Koike, N., Ohsugi, Y., Nomura, S., Yoshida, H., Nishikawa, T., Terabe, F., Ohkawara, T., Takahashi, T., Ripley, B., Kimura, A., Kishimoto, T., & Naka, T. (2008). IL-6 blockade inhibits the induction of myelin antigen-specific Th17 cells and Th1 cells in experimental autoimmune encephalomyelitis. *Proceedings of the National Academy of Sciences of the United States of America*, *105*(26), 9041–9046.
- Sheedlo, H. J., Doran, J. E., & Sprinkle, T. J. (1984). An investigation of 2':3'-cyclic nucleotide 3'-phosphodiesterase (EC 3.1.4.37, CNP) in peripheral blood elements and CNS myelin. *Life Sciences*, *34*(18), 1731–1737. [https://doi.org/10.1016/0024-3205\(84\)90572-1](https://doi.org/10.1016/0024-3205(84)90572-1)
- Shen, P., Roch, T., Lampropoulou, V., O'Connor, R. A., Stervbo, U., Hilgenberg, E., Ries, S., Dang, V. D., Jaimes, Y., Daridon, C., Li, R., Jouneau, L., Boudinot, P., Wilantri, S., Sakwa, I., Miyazaki, Y., Leech, M. D., McPherson, R. C., Wirtz, S., . . . Fillatreau, S. (2014). IL-35-producing B cells are critical regulators of immunity during autoimmune and infectious diseases. *Nature*, *507*(7492), 366–370.
- Simons, M., & Nave, K. A. (2015). Oligodendrocytes: Myelination and axonal support. *Cold Spring Harbor Perspectives in Biology*, *8*(1), a020479.
- Srinivasan, L., Sasaki, Y., Calado, D. P., Zhang, B., Paik, J. H., DePinho, R. A., Kutok, J. L., Kearney, J. F., Otipoby, K. L., & Rajewsky, K. (2009). PI3 kinase signals BCR-dependent mature B cell survival. *Cell*, *139*(3), 573–586.
- Sutavani, R. V., Phair, I. R., Barker, R., McFarlane, A., Shpiro, N., Lang, S., Woodland, A., & Arthur, J. S. C. (2018). Differential control of toll-like receptor 4-induced interleukin-10 induction in macrophages and B cells reveals a role for p90 ribosomal S6 kinases. *The Journal of Biological Chemistry*, *293*(7), 2302–2317.
- Teodorovic, L. S., Babolin, C., Rowland, S. L., Greaves, S. A., Baldwin, D. P., Torres, R. M., & Pelanda, R. (2014). Activation of ras overcomes B-cell tolerance to promote differentiation of autoreactive B cells and production of autoantibodies. *Proceedings of the National Academy of Sciences of the United States of America*, *111*(27), E2797–2806.
- Terry, R. L., Ifergan, I., & Miller, S. D. (2016). Experimental autoimmune encephalomyelitis in mice. *Methods in Molecular Biology (Clifton, N.J.)*, *1304*, 145–160.
- Trapp, B. D., Bernier, L., Andrews, S. B., & Colman, D. R. (1988). Cellular and subcellular distribution of 2',3'-cyclic nucleotide 3'-phosphodiesterase and its mRNA in the rat

- Central nervous system. *Journal of Neurochemistry*, 51(3), 859–868.
- Traves, P. G., de Atauri, P., Marin, S., Pimentel-Santillana, M., Rodriguez-Prados, J. C., Marin de Mas, I., Selivanov, V. A., Martin-Sanz, P., Bosca, L., & Cascante, M. (2012). Relevance of the MEK/ERK signaling pathway in the metabolism of activated macrophages: A metabolomic approach. *Journal of Immunology (Baltimore, MD: 1950)*, 188(3), 1402–1410.
- Weissbarth, S., Maker, H. S., Raes, I., Brannan, T. S., Lapin, E. P., & Lehrer, G. M. (1981). The activity of 2',3'-cyclic nucleotide 3'-phosphodiesterase in rat tissues. *Journal of Neurochemistry*, 37(3), 677–680.
- Wujek, J. R., Bjartmar, C., Richer, E., Ransohoff, R. M., Yu, M., Tuohy, V. K., & Trapp, B. D. (2002). Axon loss in the spinal cord determines permanent neurological disability in an animal model of multiple sclerosis. *Journal of Neuropathology and Experimental Neurology*, 61(1), 23–32.
- Xiao, B. G., Bai, X. F., Zhang, G. X., & Link, H. (1998). Suppression of acute and protracted-relapsing experimental allergic encephalomyelitis by nasal administration of low-dose IL-10 in rats. *Journal of Neuroimmunology*, 84(2), 230–237.
- Yanaba, K., Bouaziz, J. D., Haas, K. M., Poe, J. C., Fujimoto, M., & Tedder, T. F. (2008). A regulatory B cell subset with a unique CD1dhiCD5+ phenotype controls T cell-dependent inflammatory responses. *Immunity*, 28(5), 639–650.
- Yue, F., Cheng, Y., Breschi, A., Vierstra, J., Wu, W., Ryba, T., Sandstrom, R., Ma, Z., Davis, C., Pope, B. D., Shen, Y., Pervouchine, D. D., Djebali, S., Thurman, R. E., Kaul, R., Rynes, E., Kirilusha, A., Marinov, G. K., Williams, B. A., ... Ren, B., Mouse ENCODE Consortium (2014). A comparative encyclopedia of DNA elements in the mouse genome. *Nature*, 515(7527), 355–364.
- Yue, Y., Stanojlovic, M., Lin, Y., Karsenty, G., & Lin, W. (2019). Oligodendrocyte-specific ATF4 inactivation does not influence the development of EAE. *Journal of Neuroinflammation*, 16(1), 23.
- Zhang, H., & Kuchroo, V. (2019). Epigenetic and transcriptional mechanisms for the regulation of IL-10. *Seminars in Immunology*, 44, 101324.